EUROPEAN COMMISSION

Community research

FIRST-Nuclides

(Contract Number:295722)

DELIVERABLE (D-N°:5.1)
State of the art report
Update 2013

Author(s): **AMPHOS21+KIT-INE**

Reporting period: e.g. 01/01/2012 – 30/06/2013

Date of issue of this report: **31/08/2013**

Start date of project : **01/01/2012** Duration : 36 Months

DISTRIBUTION LIST

Name	Number of copies	Comments
Mr. Christophe Davies (European Commission)	One electronic copy submitted via participant portal	
All consortium members and European Commission	One electronic copy available on the FIRST-Nuclides webportal	

Project co-funded by the European Commission under the Seventh Euratom Framework Programme for Nuclear Research &Training Activities (2007-2011)		
Dissemination Level		
PU	Public	X
RE	Restricted to a group specified by the partners of the [FIRST-Nuclides] project	
CO	Confidential, only for partners of the [FIRST-Nuclides] project	

TABLE OF CONTENTS

LIST OF FIGURES

LIST OF TABLES

The 7th Framework Pogramme Collaborative Project FIRST-Nuclides: State-of-the-Art and Rationale for Experimental Investigation

Bernhard Kienzler[+], Volker Metz[+],
Ernesto González-Robles Corrales[+], Vanessa Montoya*, Alba Valls* Lara Duro*
[+]Karlsruhe Institute of Technology (KIT), Institut für Nukleare Entsorgung (INE), Karlsruhe, Germany
*Amphos 21 Consulting S.L., Barcelona, Spain

Abstract

The Deliverable D5.1 – State of the Art report is the main outcome of the documentations task within WP5 of the FIRST-Nuclides project. The first version of the State-of-the-Art was reported at the beginning of the project and it provides a view on basic information related with the spent nuclear fuel (SF) and the fast/instant release fraction (IRF) studies done in the past decades. A description of different type of spent fuels, processes induced during SF irradiation or the modelling tools used for fuel performance are included in the basic information section. The second part of the report includes a summary of more than 100 published experiments which have used different samples, experimental techniques, experimental conditions, type of solutions, etc. This report has been updated after the second year of the project.

The final version of this deliverable not only includes an update of the report with a summary of the results obtained in the project, extensively reported in the different deliverables, annual workshop proceedings and final scientific report (D.5.13), but also a database compiling data on IRF of relevant radionuclides from the spent fuel. This database is called "IRF Database".

The main aim of the IRF Database development is to make available all dissolution based fast/instant release data achieved within CP FIRST-Nuclides as well as previously published data. The data are compiled and can be used both for scientific purposes and for application in safety analyses. The studies compiled in the database have been performed under different experimental conditions, using different type of fuels, different sample preparations and different solutions.

1. Introduction

Safety assessment of the repository for spent UO_2 fuel requires that the potential release of radioactivity upon breaching of the engineered barriers system due to degradation processes be quantified.

The Fast/Instant Release fraction (IRF) of spent nuclear fuel (SF) is an operative definition arising from early spent nuclear fuel leaching experiments and it entails all those nuclides that as a result of the neutronic and thermal fields in the reactor have migrated towards the surface of the spent fuel and are easily accessible to water.

The definition of Fast/Instant Release Fraction was initiated in the 80's during the early days of the Spent Nuclear Fuel workshops where the US, Canadian and Swedish programs shared their experiences in informal annual meetings. In this context, the US and Canadian programs did a substantial amount of experimental work that will be analysed in the data section.

The IRF was incorporated in the frame of the safety assessment of spent fuel disposal in the safety assessment exercises (SA) performed at the beginning of the 90's, particularly in SKB91 (SKB, 1992). In this SA exercise the release of a number of fission products (I and Cs) was assumed to be, neither limited by the dissolution of the UO_2 matrix itself, nor by their own solubility and, in this respect they were assumed to be released instantly when water was put in contact with the spent fuel.

Other national programs became members of the Spent Nuclear Workshop during the 90's and they adopted this terminology in their approach to spent fuel dissolution. The operational basis of the Fast/Instant Release Fraction bears in itself some intrinsic limitations in the way they are treated in PA related modelling. This is highly unsatisfactory from the scientific and technical perspective as it unreasonably penalizes spent fuel disposal from the radiological point of view. Under this perspective it is highly advisable that a more scientific and consistent approach is developed to characterize and model the potential release of these fission products.

From the point of view of performance assessment (PA) of the repository for spent fuel, the fast/instant release fraction is the fraction of the radioactive inventory that will be released from the waste "immediately" after the fuel rod cladding fails, and the waste containment is compromised. The FRF may have important implications for PA because some of the preferentially released radionuclides are characterised by both relatively long half-lives and high degrees of mobility (e.g. ^{129}I and ^{36}Cl (Johnson et al., 2012)). As a result, a great deal of effort has been directed into improving the understanding and quantifying the physico-chemical processes involved in the instant release of radionuclides from SNF. These goals are being achieved through a combination of experimental and modelling work (Johnson et al., 2004, 2005, 2012, Ferry et al., 2007; Lovera et al., 2003; Poinssot et al., 2005; Grambow et al., 2010)

In-reactor irradiation with neutrons causes a continuous production of fission products within the fuel. The fission products include isotopes of noble gases (mainly Xe and Kr) and others, such as ^{3}H, ^{14}C, ^{79}Se, ^{99}Tc, ^{107}Pd, ^{125}Sn ^{129}I, ^{135}Cs, and ^{137}Cs. Fission products (FP) may occur in the fuel as i) volatiles (I, Br, Cs, Rb, Te), ii) metallic precipitates (Mo, Tc, Ru, Rh, Pd, Ag, Cd, In, Sn, Sb, Te), iii) oxide precipitates (Rb, Cs, Sr, Ba, Zr, Nb, Mo, Te) or iv) oxides in the

UO_2 structure (Cs, Nb, Te, Y, Zr, the earth alkaline elements Sr, Ba, Ra and the lanthanides La, Ce, Pr, Nd, Pm, Sm, Eu) (Kleykamp, 1985).

In a rod containing stacked pellets of polycrystalline UO_2 fuel during reactor operation, concentration and thermal gradients drive diffusive redistribution of some of the fission products into the inter-granular space, and outside the pellet towards the inner-rod void space. It is thought that under repository conditions, breaching of the cladding would lead to a rapid release of the inventory accumulated in the void space of the rod. Also, some radionuclides segregated at the fuel grain boundaries would be released relatively quickly. Both of these inventory fractions are typically considered to constitute the IRF. In contrast, a much slower radionuclide release would occur over long periods of time due to dissolution of the UO_2 matrix (Johnson et al., 1997, 2005)

Fast Release Fraction has been the objective of investigations since the early days of spent fuel investigations. In addition, the fast / instant release of radionuclides from spent nuclear fuel has been investigated in a series of previous European projects (such as SFS (Poinssot et al., 2005), NF-Pro (Sneyers et al., 2010), MICADO (Grambow et al., 2010)). Furthermore, mainly French research programs investigated and quantified the rapid release.

In this context, the 7th Framework Programme Topic Fission-2011-1.1.1 "research activities in support of implementation of geological disposal", the Collaborative Project (CP) Fast / Instant Release of Safety Relevant Radionuclides from Spent Nuclear Fuel (FIRST-Nuclides) aims to bring about a more scientific basis to the understanding and the modelling of the release of these initially easily dissolving nuclides. The CP started in January 2012 and has extended over 36 months. The objectives of the project are in line with the Vision Report and the Strategic Research Agenda (SRA) of the "Implementing Geological Disposal – Technology Platform (IGD-TP)".

Six experimental facilities having specialized installations and equipment to work with highly radioactive materials and four organizations having specific knowledge on this subject have entered into an Inter-European collaboration with the aim of investigating the behaviour of spent nuclear fuel during the first step of their interaction with water and providing additional rationale for the understanding of the processes involved. The experimental facilities will perform studies using high burn-up spent nuclear fuels and will use a combination of advanced analytical methods to characterize its dissolution behaviour.

The beneficiaries of the consortium are the following organizations: Karlsruher Institut fuer Technologie (KIT) DE, Amphos 21 Consulting S.L. (AMPHOS21) ES, Joint Research Centre – Institute For Transuranium Elements (JRC-ITU) EC, Forschungszentrum Juelich GMBH (JÜLICH) DE, Paul Scherrer Institut (PSI) CH, Studiecentrum voor Kernenergie (SCK•CEN) BE, Centre National De La Recherche Scientifique (CNRS) FR, Fundacio Ctm Centre Tecnologic (CTM) ES, Magyar Tudományos Akadémia Energiatudományi Kutatóközpont (MTA EK) HU, Studsvik Nuclear AB (STUDSVIK) SE. Associated groups, contributing also to FIRST-Nuclides with their experiences and having access to the discussions within the

project are: Commissariat à l'energie atomique et aux energies alternatives (CEA) FR, Los Alamos National Laboratory (LANL) USA, Sandia National Laboratory (SNL) USA, National Decommissioning Authority (NDA) UK, National Nuclear Laboratory (NNL) UK, Posiva Oy FI, Teollisuuden Voima Oy (TVO) FI, Gesellschaft für Anlagen- und Reaktorsicherheit mbH (GRS), DE, University of Cambridge, Department of Earth Sciences UK, Centro de Investigaciones Energéticas, Medioambientales y Tecnológicas (CIEMAT) ES, The Centre for Nuclear Engineering, Imperial College, London UK, Divize Chemie palivového cyklu a nakládání s odpady/Fuel Chemistry and Waste Disposal Division (ÚJV Řež) CZ and Lancaster University UK

The outcome of abundant research on instant release fraction characterization and dissolution has clearly put in evidence the relationship between, fuel burn-up, fission gas release (FGR) and Cs content in the gap. However, there are still some open questions, which were pointed out during the MICADO project (Grambow et al., 2010). Among them the most critical ones would be:

- To define more realistic relationships between FGR and the presence of fission products in the gap, including C, Rb, Sr, I and Tc
- The quantification of the IRF in high burn-up fuels
- The role of grain boundaries in the potential retention of fission products.

A recent publication (Johnson et al, 2012) brought some additional data from higher burn-up fuels that indicated that the basic relationships between FGR and Cs release were maintained and that the I release was closely related to FGR. Nevertheless, not sufficient data are available and significant correlations between sample preparation and IRF quantification seem to exist.

The project FIRST-Nuclides aims at contributing to find a satisfactory answer to the former questions. The present report summarises the state-of-the-art after the finalisation of the project and shows the rationale for the investigations undertaken within the project, based on expensive experiments using irradiated nuclear fuels in hot cell facilities and application of sophisticated analytical methods and modelling tools.

Giving the long-term needed for this type of investigations and the time needed to obtain clearance for the use of the data from the nuclear electricity operators, some of the investigations have been set up but have not yet provided all the desired data at the end of the project. In agreement between the partners of the project, these experiments have not been stopped, and they will still be running in order to provide further experimental evidences to understand the fast release processes. The present report summarises the data obtained from the project at its formal end, i.e., December 2014.

2. Description of the fuel

There are three main stages in the fabrication of the nuclear UO_2 fuel used in Light Water Reactors (LWR) and Pressurized Heavy-Water Reactors (PHWR):

1. Production of pure uranium dioxide (UO_2) from UF_6 or UO_3.
2. Production of high-density ceramic UO_2 pellets.
3. Production of the material for the encapsulation of the fuel pellets and preparation of the fuel assembly – mainly from zirconium alloy; and loading the fuel pellets into the fuel rods, sealing them and assembling the rods into the final fuel assembly structure.

UO_2 pellets

UO_2 powders are compacted by means of high loads (several hundreds of MPa) and sintered with sintering aids to an initial density of 4.5-5 g cm^{-3}. (see Figure 1). The sintering is performed at ~1700 °C for 2 to 8 hours under reducing atmosphere, normally Ar-H_2. The grain size of this material can be adjusted by adding additives to the powders such as Cr_2O_3. The grain size influences both the mechanical properties and the fission gas release (FGR) of the fuel. Larger grains show a lower FGR. Some additives produce a coating onto the outer surfaces of the grains what reduces the FGR further. Additives up to 50,000 ppm of metal oxides can form oxygen defects, which can incorporate fission gases. During the sintering process, the remaining U(VI) is reduced. Present UO_2 fuels have grain sizes of 10-20 µm, a density of 10.0 to 10.8 g cm^{-3} and pore sizes in the range of 0.5 to 80 µm.

Figure 1. From powder to pellet. A) Powder: UO2 grain size of 20 µm; B) Pellet: PWR 17×17 - ∅ 8.17 (AREVA) - a length of 9.8 mm, BWR 10×10 - ∅ 8.87 (Atrium 10XP) - a length of 10.5 mm.

MOX fuel is a mixed uranium oxide + plutonium oxide which has been used in some reactors in Europe and Japan. It consists on depleted uranium (about 0.2% in ^{235}U) coming from the

enrichment of uranium, and plutonium oxides from the processing of spent nuclear fuel. The pressing and sintering process is very similar to the one of UO_2 pellets although some additional protection is needed in order to avoid exposition to spontaneous neutron emissions from ^{234}Pu.

Optimization of nuclear fuel (UO_2)

As previously mentioned, with the aim of enhancing the economical efficiency of the nuclear generation cycle, and to reduce the amount of spent fuel, the fuel discharged burn-up has been increased in the last years. This is the reason why research on fuel pellets focuses more and more on the high burn-up fuel pellets.

The utilities have put in place a number of improvements to optimize the performance of the UO_2 fuel during operation. Some of them have clear consequences in the fission gas release (FGR) and fission product generation. The optimization of the nuclear fuel covers a series of different processes:

- The initial enrichment with respect to increased burn-up,
- The control of criticality,
- The burn-up behaviour, such as swelling
- The mechanical and thermal requirements,
- Pellet cladding interactions (PCI)
- Minimization of fission gas release by adjusting UO_2 grain sizes, grain pores, and grain coverage.

Most of these optimizations are only described in patents. For example, for criticality control, some rods in the fuel elements are doped with Gd. In BWR fuel elements between 1 and 18 rods are doped between 1 and 7 wt.%. In PWR fuel elements between 2 and 12 rods are doped with Gd_2O_3 in the concentration range between 1 and 7 wt. %. The manufacturing process of these binary oxide fuels was published by Assmann et al. (1998).

The mechanical and thermal behaviour of the fuel, the UO_2 grain sizes and grain pores are controlled through the sintering process. Various sintering processes have been described (mainly in patents). One example is the NIKUSI low temperature process. The "NIKUSI" process bases on a two steps low temperature sintering technique for UO_2 involving sintering at 1100 to 1200°C in CO_2 and later reduction in hydrogen (Assmann, 1986).

A higher burn-up in the fuels, leads to an increase in the amount of fission gases such as xenon (Xe) and krypton (Kr). The fission gases in the pellet are continuously released out from the pellets during the reactor operation and increase the internal pressure of nuclear fuel rod. The increased internal pressure induced by the nuclear fission gases increase the stress working on the cladding tube, and as a consequence reduces the safety margin of the nuclear

fuel rod. To minimize these problems, the nuclear fission gases generated due to nuclear fission must be released out in as small amounts as possible from the sintered pellet.

In the last years, different conceptual models are accounted for to explain the release of the gas from the fuel pellet, and for a complete description of the different concepts and models developed to account for FGR the reader is referred to deliverable D.4.2. of the FIRST-Nuclides project, which can be accessed in the project website. The process of nuclear fission gas release to the outside of the nuclear fuel pellet is generally conceptualised in a way than when the fission gas is generated in a grain, it moves to the grain boundary through diffusion so as to exist as bubbles in the grain boundary, and when the bubbles are increased to reach a certain amount, a bubble tunnel is formed along the grain boundary, and the bubbles are then discharged to the outside of the nuclear fuel pellet. Therefore, the larger the grain size of the pellet, the longer the time needed for the gas to reach the grain boundary, thus to be released. This means that a high burn-up fuel would require a larger grain size to minimize gas release.

Admixtures of various metal oxides control the evolution of mono-disperse grain size during sintering (Gradel et al., 2004; Bastide et al., 1993). The pore structures and pore sizes of uranium dioxide fuel can also be varied by application of precursor liquids, for example, alylhydridopolycarbosilane (AHPCS) before sintering (McCoy et al., 2010). Current high burn-up fuel has grain sizes between 20 and 25 µm. Covering the UO_2 grains by various ceramic compounds described in some patents can also minimize FGR. If, and to which extent, such specially treated UO_2 is used by the utilities is regarded uncertain as it belongs to the realm of utilities operational know-how.

A low density of the material, on another hand, may enhance fission gas release. This effect has been observed from experiments reported in Johnson et al. (2012), when comparing the results of FGR obtained from fuels of a density of 10.05-10.3 g/cm^3 instead of the usual denser fuels (10.5 g/cm^3).

Fuel Rods and fuel elements

Nuclear fuel assemblies are complex engineered products, made according to the individual specifications of each customer. The main specifications are given by the physical characteristics of the reactor, by the reactor operating and fuel cycle management strategy of the utility, as well as by national licensing requirements. Most of the main fuel fabricators are owned by reactor vendors, and they usually supply the initial cores and early reloads for reactors built to their own designs.

The light water reactor (LWR) is a nuclear power reactor initially developed in the USA. The power reactor is filled with normal water. This water cools the power reactor and moderates the neutron energy to help the nuclear fission. There are two main types of reactors: the pressurized water type (PWR) and the boiling water type (BWR). The LWR fuel element,

both for PWR and BWR, consists of a quadratic arrangement of fuel and control rods (except the PWR VVER, which presents an hexagonal arrangement) (see Figure 2).

A **fuel rod** itself consists of a gas-tight Zircaloy/M5 cladding and has end caps in both ends. At the bottom there is a supporting sleeve. Above, an insulating pellet of Al_2O_3 separates the supporting sleeve from the uranium dioxide pellets. The UO_2 pellets are stacked up to the heights of the reactive zone of the reactor. Also at the top of the fuel rod, an Al_2O_3 insulating pellet separates the UO_2 pellets from the fission gas plenum, which contains a pressure spring. The spring keeps the pellets in place while reserving some space inside the rod for volume expansion as the pellets expands due to heat and neutron irradiation, and because of formation of gaseous fission products. The fuel rods are filled with He gas to a pressure of 22 bar. At the top and bottom, the rods are fixed by an anchor grid, between top and bottom the rods distance between the rods is fixed by spacers. The rod material consist of Zry-2 partly Fe enhanced for BWRs and of M5, Optimised Zry-4, modified Zry-4 or Duplex (Fuel suppliers, 2004) for PWRs.

A **fuel element** consists of the fuel rod, spacers and control rods. The nuclear fuels to be considered in the CP FIRST-Nuclides are originated from, mainly pressure water reactors (PWR and VVER-440) and boiling water reactors (BWR). An overview of relevant fuel element types is given by (Fuel suppliers, 2004), where four main reactor types (PWR, VVER, BWR and heavy water) are represented. Illustrations and photographs show the representative designs for most of the manufacturers. AREVA produces PWR fuel elements arranged in a square, holding 14x14-(16+1) 15x15-(20+1) 16x16-(20) 17x17-(24+1) to 18x18-(24) fuel rods, for BWRs the ATRIUM fuel elements have 9x9 and 10x10 designs. A cross cut through a BWR fuel element (Olkiluoto, OL1/2, Findland) is given in Figure 3, showing the arrangement of the two water rods for improvement of moderation and the twelve gadolinium doped rods (TVO). These rods are required for high burn-up, where higher initial ^{235}U enrichment is used. For new fuel elements, a reduction of the power peaking factor and a compensation of the excess reactivity is achieved by the burnable neutron poison, Gd. Gd may be incorporated (as oxide) into the fuel pellets of some rods to limit reactivity early in the life of the fuel. It has a very high neutron absorption cross-section and competes strongly for neutrons, after which they progressively ‘burn-out’ and convert into nuclides with low neutron absorption leaving fissile (^{235}U) to react with neutrons. Burnable absorbers enable longer fuel life by allowing higher fissile enrichment in fresh fuel, without excessive initial reactivity and heat being generated in the assembly. Some fuel elements have radially zoned enrichment distributions, which reduce the power peaking factor and optimize the heat transfer.

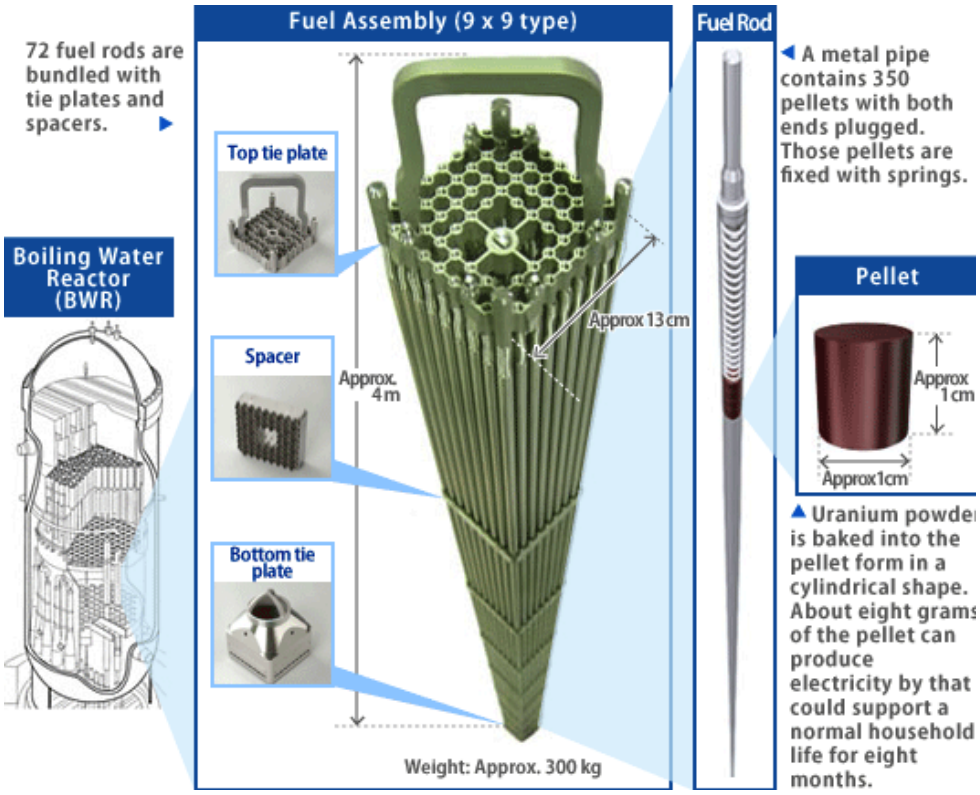

a) Scheme of a BWR reactor, fuel assembly, rod and pellet

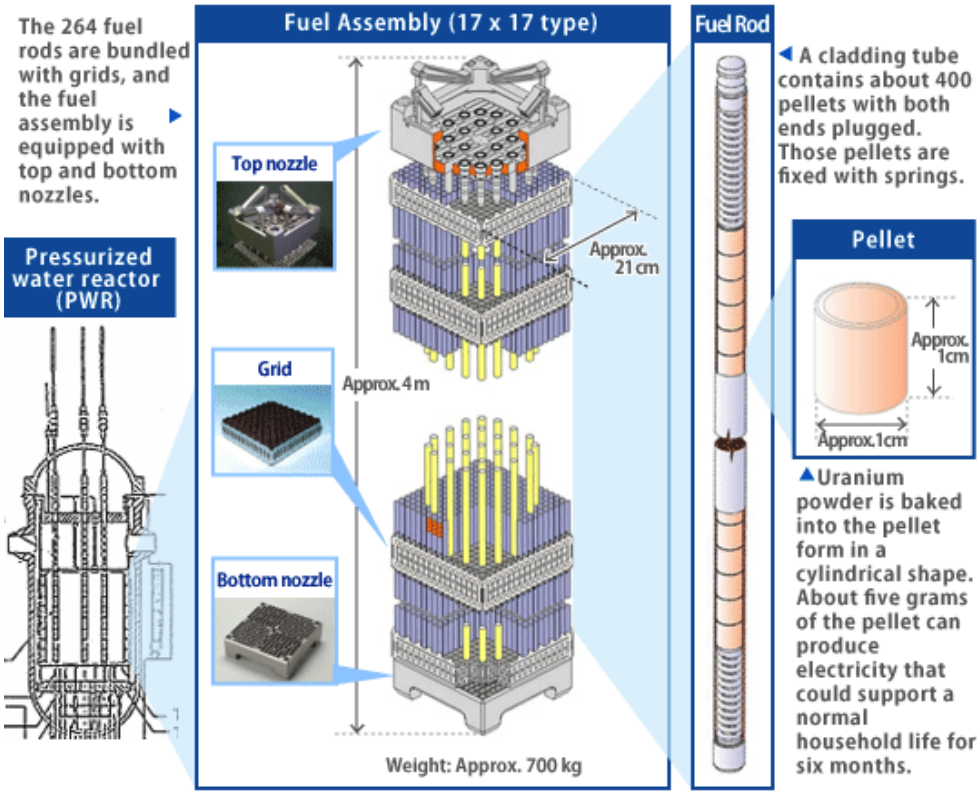

b) Scheme of a PWR reactor, fuel assembly, rod and pellet

Figure 2. Schemes of BWR (a) and PWR (b) fuel assemblies, fuel rods and pellet characteristics. Taken from http://www.nfi.co.jp/e/.

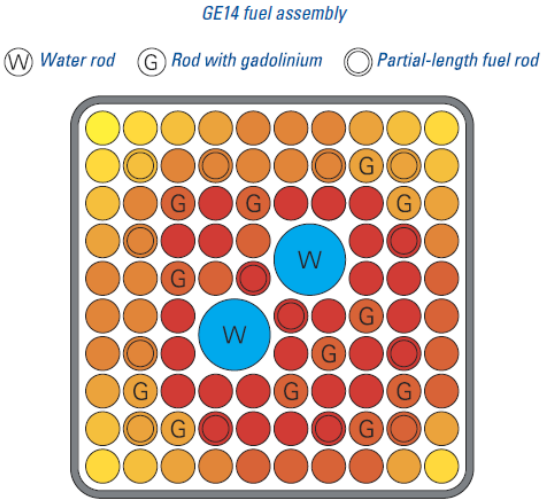

Figure 3. Arrangement of radially zoned fuel rods, Gd2O3 doped rods and water rods in a 10×10 OL1/2 BWR fuel element.

The fuel rods may have many different levels of enrichment zones and burnable absorbers. It is not uncommon to have ten or more different fuel rod designs in a single assembly. It is very important that a fuel rod of a given design be located in its designed position in the assembly (Deshon et al., 2011).

Disposal of spent nuclear fuel

While the abundance and composition of fission products and fission gas release is highly dependent on the fuel fabrication and reactor operational factors, the fast release fraction is only relevant in the frame of the disposition of the used fuel. It is a very important and critical component of the performance of spent fuel storage facilities, but it is also very relevant when assessing the performance of spent fuel geological repositories. In this context, we will give a brief account of the commonalities in European disposal concepts and how they affect potential dissolution behaviour of the SF, and the fast release of the fission products.

Canister concepts

All European disposal concepts for spent nuclear fuel consider thick-walled inner steel casks having various overpack or other protecting properties. The different /canister disposal concepts are described in Appendix II.

Water contact to the fuel in the casks

Under disposal conditions, one may assume that after a certain period of time water penetrates into the inner steel cask and starts corroding the steel at the inner steel surfaces causing a hydrogen pressure build-up due to anoxic steel corrosion. Some corrosion mechanisms are shown in Appendix II.

Water access to the spent fuel

The potential barrier function of the Zircaloy cladding of the fuel rods is not considered in current assessments but the behaviour of this material may affect the instant/fast release of radionuclides from the spent fuel. An irradiated cladding can contain local hydrogen concentrations higher than 1000 ppm. The embrittlement effect of hydrogen in Zircaloy is far less at 350°C than that at lower temperatures e.g. 100°C (Rudling et al., 2008). Under the assumption that water penetrates into the canister, anaerobic corrosion of the steel starts forming hydrogen gas. The gas dissolves in the contacting water until its solubility is exceeded. A gas phase can be form afterward, and the gas pressure increases until an equilibrium pressure is achieved which depends on the depth of the repository. At 500 m depth, the maximum pressure is in the range of 5 MPa. This may cause further penetration of H_2 into the Zircaloy. Detailed studies of the H_2 effect on the Zircaloy embrittlement are available, e.g. (Varias et al., 2000; Bai et al., 1994; Chan et al., 1996). Due to the homogeneous distribution of H_2 over the length of the fuel rods, embrittled material zone extends over the complete length of the rods. Therefore, it can be expected that the cladding of the fuel rods will not be damaged by single holes (such as pitting corrosion in stainless steel) but by ruptures, especially at positions where pellet cracking occurred. Maximal cladding hoop stress is located between pellets. Such defects have been investigated in the context of Pellet Cladding Interaction studies (Cox, 1990; Marchal et al., 2009). A schematic view is given in

Figure 4.

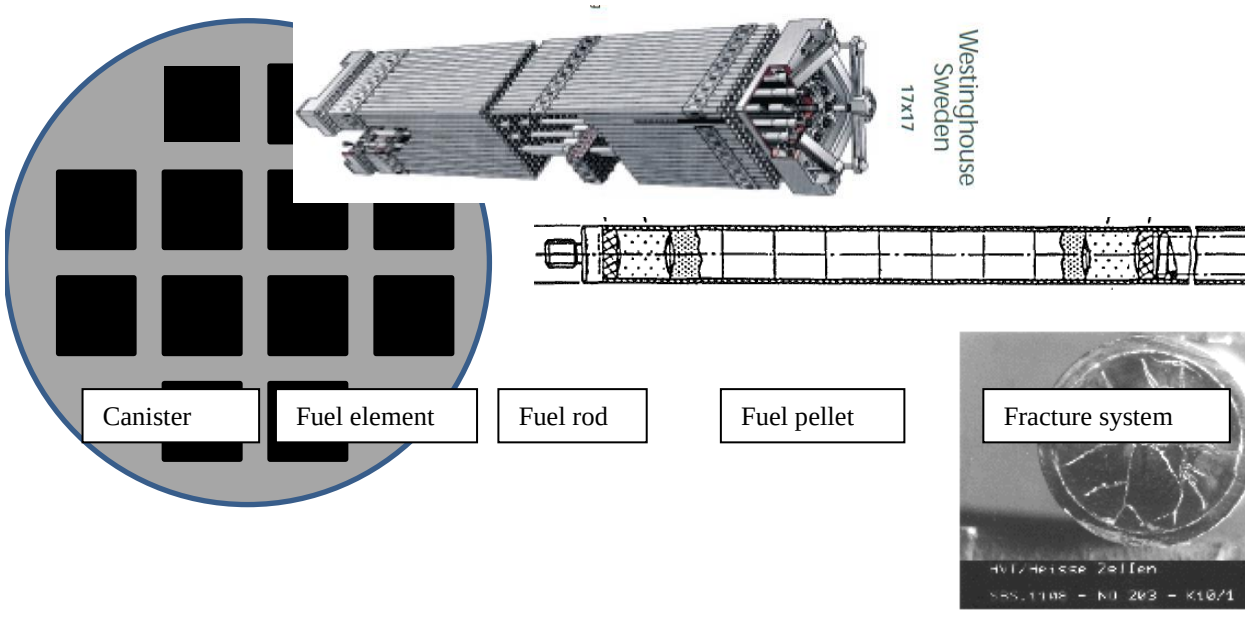

Figure 4. Pathways for water/solution access to the spent fuel under disposal conditions.

3. Irradiation induced processes in UO_2

The abundance and generation of fission products are the result of the irradiation processes in the fuel. Originally UO_2 fuel is fabricated by pressing and sintering the powder to a density less than 100% of the theoretical density due to pores in the bulk material. During a burn-up in the range of ~50 GWd/t_{HM}, the FIMA (Number of fissions per initial metal atom) is about 5.5 atom-%. The fission and fission products cause expansion in the UO_2 crystal structure leading to swelling (Stehle et al., 1975).

The status of the spent nuclear fuel when discharged from the reactor can be schematized by Figure 5a, taken from Johnson and McGinnes (2002). In the figure, four different areas are differentiated in the fuel rod, presenting different radionuclides:

- The gap and the free volumes of the rod, including open porosity
- The rim (external) zone, presenting a small grain size and low porosity
- The grain boundary
- The grains of the UO_2 matrix

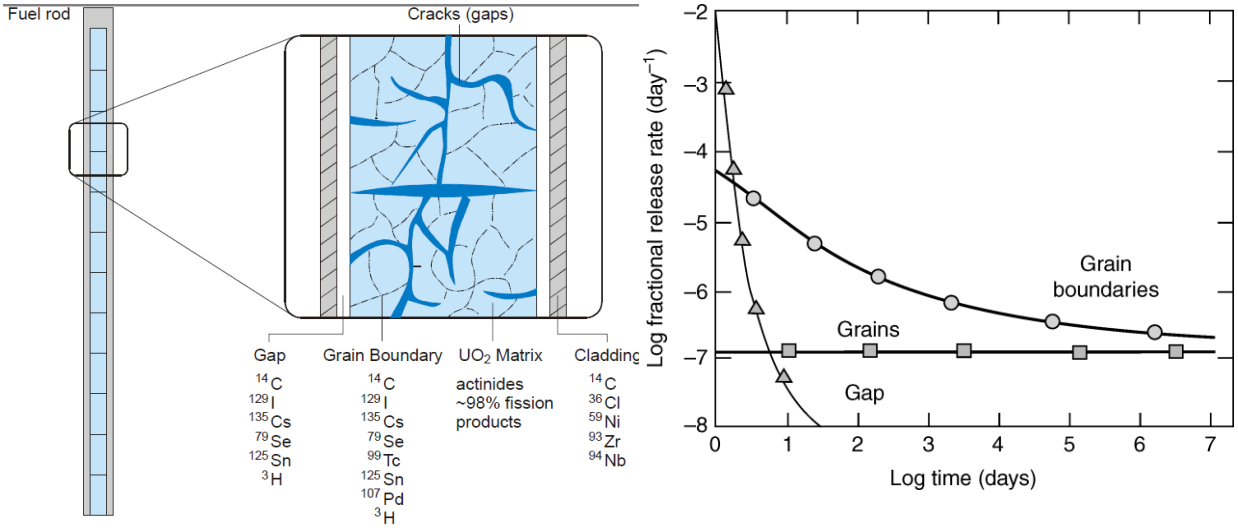

a) b)

Figure 5. a) Different zones of the fuel and radionuclides distribution (from McGinnes, 2002) and b) Fractional release rates for radionuclides located at different zones of the fuel (from Johnson, 1985).

Johnson (1985) proposed different release rates for different fuel compartments (Figure 5b), showing the lower release rate of radionuclides located in the grains of the matrix, the release from the gap, which is faster, i.e., radionuclides are not bound but easily released in the gap and open porosity, and finally those radionuclides in the grain boundaries, which present an initial faster release rate which decreases with time to reach that of the grains.

Each pellet is fragmented after irradiation, what affects importantly to the structural, physical and chemical properties.

Initial porosity reduces pellet swelling. Swelling is a consequence of the fission process increasing the number of atoms thus affecting the physical/chemical properties of the fuel. A high initial porosity is helpful from this point of view but it has other consequences, for example:

- Porosity influences all the physical properties of the fuel, e.g. thermal conductivity, creep and strength, and elastic constants.
- Porosity influences moisture and residual gas content of the pellets.
- It may produce overcompensation of the swelling during the early reactor irradiation causing rapid shrinkage of small sized pores and a densification of the UO_2.

UO_2 spent fuel stoichiometry and composition.

The face-centered cubic UO_2 shows an extended range of composition apart from the exact stoichiometry O/U = 2, and the material is referred to as $UO_{2\pm x}$. The deviation x from the stoichiometric composition affects all physical and chemical properties, in particular those which depend on the atomic mobility (e.g. diffusion coefficients), and the oxygen partial pressure or chemical behaviour of the fission products.

The chemical stability of *oxides of the fission products* in the spent nuclear fuel $UO_{2\pm x}$, can be classified into two groups, according to Kleykamp (1985) and later refinements:

- Fission products forming oxide precipitates (Rb, Cs, Sr,Ba, Zr, Nb, Mo, Te); these oxides tend to have the general composition AB[O3] and to adopt a cubic perovskite-type structure with Ba, Sr, and Cs in the A sites and Zr, Mo, U and lanthanides (Ln) in the B sites
- Fission products occurring as oxides in the UO2 fuel matrix (Cs, Nb, Te, Y, Zr, the earth alkaline elements Sr, Ba, Ra and the lanthanides La, Ce, Pr, Nd, Pm, Sm, Eu). Zr and rare earth elements are partially or completely miscible with UO2 to form a solid solution.

Fabrication imperfections

There are a number of potential fission processes that may arise as a result of defects and failures in the fabrication of the fuel pellets. The most interesting in relation to FIRST-Nuclides project are the so-called pellet to cladding interactions. Pellet to cladding mechanical interaction is associated with a defect in the pellet or cladding, such as a missing pellet surface (MPS), which creates excess stress in the cladding. Rapid changes in local power cause pellet

expansion, which, in the presence of these stress multipliers, can break the cladding. The other type of pellet cladding interaction is stress corrosion cracking. High power levels promote the release of fission product gases. Iodine in particular is very corrosive to Zircaloy. The presence of iodine near a pre-existing cladding imperfection or a stress riser accelerates crack propagation through stress corrosion cracking. PCI can also occur during reactor startup due to rapid changes in core power and unconditioned cladding.

Thermal processes during operation

The UO_2 pellets are subject to a high central temperature and a steep radial temperature gradient. Like other ceramic materials, UO_2 shows little thermal shock resistance and behaves in a brittle manner at low temperatures. The vapour pressure increases rapidly with temperature. These properties are responsible for the development of a typical crack pattern in the cool outer part of the pellets and micro-structural changes in the hot inner part of the pellets, up to a complete change in microstructure without melting.

The actual temperature, stresses and behaviour of fuel rods under irradiation are modeled by 2D or 3D codes (Rashid et al., 2011). For a rough estimation, an analytical equation may be used which relates the linear power to the temperature increase ΔT of a fuel rod.

$$\Delta T = \frac{lin.power}{4\pi \cdot \lambda} \qquad \text{eq. 1}$$

Using eq. 1 following temperatures are obtained for different reactors (Table 1) (The heat conductivity $\lambda_{irrad\ fuel}$ = 2.5 W m^{-1} K^{-1} was used (Lucuta et al., 1996).

Table 1. Temperatures obtained for different reactor fuels by applying equation 1.

Pellet	KKG (PWR)	GKN II (PWR)	KKL (BWR)
∅ [mm]	9.3	8.05	8.5
Lin power [W/cm]	228	167	184
ΔT [K] (eq.1)	725	528	585
$T_{coolant}$ [K]	325	305	263
T_{center} [K]	1050	833	848

During the operation in a reactor, the temperature causes a radial thermal expansion of the fuel pellets, which is partly reversible when cooling.

Relationship between fuel enrichment and burn-up

The resulting fission product generation and consequently the composition and abundance of fission products is related to the fuel history and burn-up. In this respect, there is a correlation between initial fuel enrichment and burn-up. In the early days of nuclear power generation average burn-up values ranged between 30-50 GWd/t_{HM}. In the last years, with the aim of increasing cost efficiency and decrease spent fuel volumes to manage after burn-up in the reactor, the discharge burn-up has increased.

In 2003 the OECD/NEA Nuclear Science Committee initiated an Expert Group on Very High Burn-ups in LWRs, with the task of delivering a state-of-the-art report on high burn-ups in LWRs. Very high discharge burn-ups are defined by this group, as average burn-ups from 60-100 GWd/t_{HM}. The 60-100 GWd/t_{HM} range took the analysis largely beyond the usual range of current LWR experience (although there was experience of experimental test rods having been taken into this burn-up range) and looked very much to the future of LWRs. The report covered only conventional LWR fuel assembly designs, which conform to the assembly geometries used in present LWRs and that use conventional oxide fuels (NEA, 2006). Figure 6 shows the initial ^{235}U enrichment versus the average discharge burn-up.

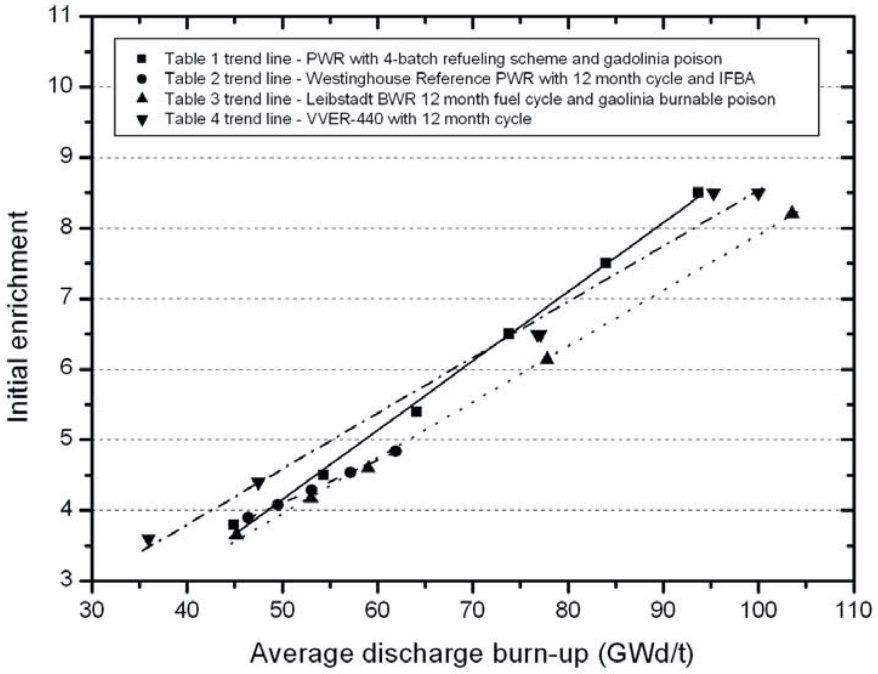

Figure 6. Initial ^{235}U enrichment versus average discharge fuel burn-up (NEA, 2006)

The initial enrichment relation in Figure 6 indicates that the maximum average discharge burn-up achievable within the 5.0 wt.% ^{235}U fabrication limits is slightly above 60 GWd/tHM. This figure may be slightly pessimistic because of the gadolinium residual absorption penalty and because a five- or six-batch scheme or higher (instead of 4 cycles) are known to yield slightly higher average discharge burn-ups for the same initial ^{235}U enrichment.

As example, the following information can be useful: In BWR from the Leibstadt powerplant (BWR-KKL) the fuel pellet enrichment varies between 4.46 and 3.71% ^{235}U and density of 10.50 and 10.53 g cm^{-3} respectively. The average grain size is 10–11 µm (Leddergerber et al., 2008). In PWR from the Gösgen plant (PWR-KKG), the initial ^{235}U enrichment in UO_2 fuel rods is presently 4.5-5.0 % ^{235}U. In the PWR from the Neckarwestheim-II reactor (PWR-GKN II), the enrichment is 4.4 wt.% for fresh UO_2 fuel and 4.6 wt.% for UO_2 fuel produced from reprocessed uranium.

4. Modeling tools for fuel behaviour

Models for Fuel Performance

The morphology of the fuel pellet, the properties of uranium oxide, its structure, thermal expansion and thermal conductivity and heat capacity affect the performance of nuclear fuel. The properties of the cladding materials have to guarantee compatibility of the UO_2 fuel with respect to thermal properties, linear thermal expansion, thermal conductivity, specific heat capacity and the mechanical properties, including the elastic constants and the plastic deformation properties. They account also for irradiation effects, such as irradiation-induced growth and hardening, as well as irradiation-induced creep behaviour. The corrosion and hydrogen pickup of the cladding are also important parameters especially under the high temperature conditions in a reactor. All these processes are accounted for in modelling tools currently used by the utilities to simulate and predict fuel behaviour during reactor operation.

Modelling tools take into account basic phenomena for in-reactor performance, such as the neutronics of the fuel, the evolution of the nuclide content and the presence of absorbers. They also take into consideration all heat transfer processes and the thermal characteristics under consideration of the axial heat transport in the coolant, the heat transport in the pellet, the heat transport through the cladding. The effects of irradiation on gap conductance between the pellets and cladding are also considered. The modelling of the mechanical behaviour includes the calculation of strains in the pellet and cladding. Further modelling tools have been developed for studying the fission gas behaviour, for modelling the high burn-up structure, pellet-cladding interaction, irradiation-induced stress corrosion cracking and cracking events caused by power ramps. Additionally, a series of codes deal with accidental situations in a reactor core. A comprehensive summary of the relevant basic assumptions and equations are provided by Van Uffelen et al. (2010) in the recent published Handbook of Nuclear Engineering.

The utilities and manufacturers of nuclear fuel use a number of different codes. A special issue of the journal “Nuclear Engineering and Design” collected the papers from the IAEA Specialists' Meeting on the Computer Modelling of Nuclear Reactor Fuel Elements, held March 13-17, 1978 at Blackpool, UK (Vol. 56 (1) 1980). Various specialists meetings and workshops have been organized, for example by IAEA (2001) and NEA. A recent overview on Fuel Performance Codes was published by Stan (2009). Dion Sunderland; Nuclear Science and Technology Interaction Program (NSTIP), ORNL, have provided the list of important codes July 8, 2011). Codes are used for different purposes, e.g. regular fuel performance, but also for “loss-of-coolant accidents (LOCA)”. They consider items such as:

- thermal-mechanical behaviour of the fuel (pellet), thermal expansion, creep effects, thermal induced porosity effects and densification, cracking
- fission induced densification and swelling, pore formation

- pellet cladding interactions (PCI),
- chemical properties such as diffusion processes for oxygen and fission products, crystal structure – defects, phase stability of nuclear fuels, especially during transient regimes,
- Fission gas release (FGR).
- A detailed description of effects relevant for FGR is given in the thesis of Peter Blair (2008).

Under the guidance of the Nuclear Science Committee (NSC) of the NEA, Multi-scale Modelling Methods are evaluated (Fig. 4). The expert group aims to provide an overview of the various methods and levels of models used for modelling materials for the nuclear industry (fuels and structural materials). The state of the art includes an overview of the methods but also the possibilities and limits of linking different scales. The report also covers the "Mixed-oxide (MOX) Fuel Performance Benchmark for the Halden reactor project MOX Rods (Tverberg, 2007).

(see http://www.oecd-nea.org/science/wpmm/expert_groups/m3.html).

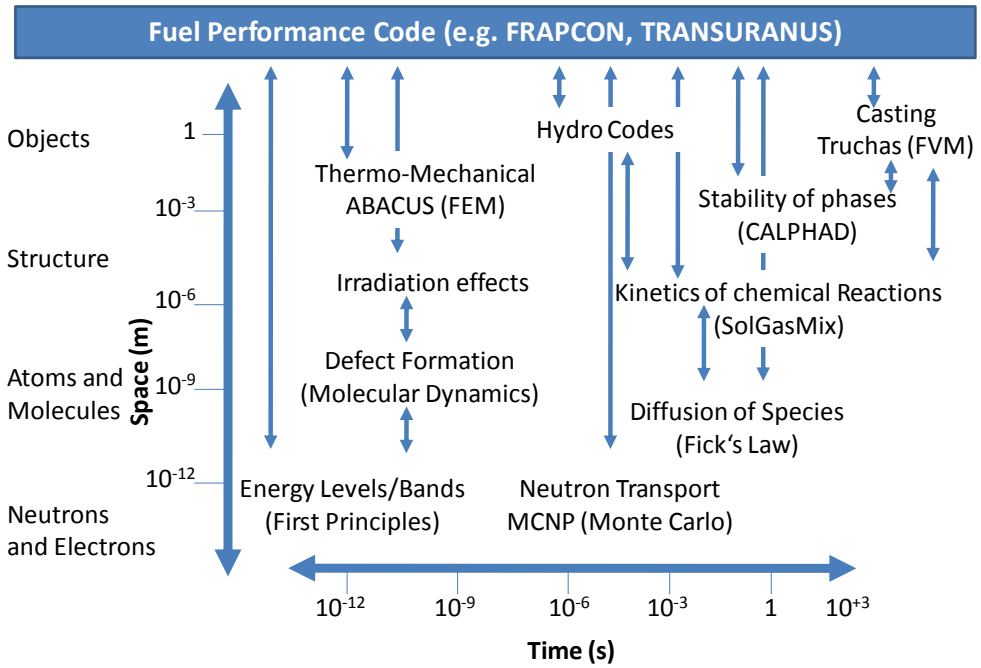

Figure 7. Space and time scales involved in simulating phenomena relevant for nuclear materials. The modelling assumptions and approaches are shown in parenthesis (Stan, 2004).

Since 2003, annual Materials Modeling and Simulation for Nuclear Fuels (MMSNF) workshops are organized. The goal of the MMSNF workshops is to stimulate research and discussions on modeling and simulations of nuclear fuels, to assist the design of improved fuels and the evaluation of fuel performance. In addition to research focused on existing or improved types of LWR reactors, modeling programs, networks, and links have been created.

Examples are organized in EURATOM 7th FP, such as the F-BRIDGE project (Basic Research for Innovative Fuel Design for GEN IV systems (www.f-bridge.eu), the ACTINET network, the EURACT-NMR coordination and support action[1] of to provide access to European nuclear licensed facilities that have recently invested in advanced nuclear magnetic resonance spectrometers.

Models for FGR and IRF

A review of the available models developed to account for fission gas release has been done during the project (see D.4.2 of the CP FIRST-Nuclides project, available from the project website for details: www.firstnuclides.eu) from where the following classification of models used to describe FRF has been obtained:

- Empirical and semi-empirical models for ***IRF***: Most empirical models rely on the observation that the quantities of radionuclides in the inner-rod void and those leached from the fuel grain boundaries correlate with fission gas release (FGR) (Johnson et al. (2004), Johnson et al. (2005), Johnson and Tait (1997), Johnson and McGinnes (2002)). These correlations can be used inversely to estimate the IRF (within the calibration range) if the FGR is known. With respect to the fission radionuclides for which there are no experimental data and no such empirical correlations exist (e.g. Cd), bounding IRF values can be defined based on consideration of their diffusion coefficient during irradiation relative to other radionuclides for which such data are available (Johnson et al., 2005).
- Empirical and Semi-empirical Models for ***FGR***: FGR can be correlated with the release of other fission products, thus providing useful information on IRF. FGR can be measured during post-irradiation inspection (PIE), but this is costly, impractical for large numbers of rods and does not offer predictive capability. Because FGR from fuel during reactor operation is an important safety and economic consideration, predictive models for this process have been in development since the early days of the nuclear power generation. In general, these models fall into two broad categories: (1) empirical and semi-empirical correlations and (2) process-oriented mechanistic models that often are incorporated into fuel performance assessment codes.
- Mechanistic Models: Fission gas generation and transport during irradiation contributes to fuel swelling and has the potential to cause damage to the cladding due to strong pellet-cladding mechanical interactions. As such, it is a significant safety consideration and considerable amount of effort has been dedicated to better understand these processes.

[1] Nuclear magnetic resonance can provide unique atomic scale structural information in liquids and crystalline and amorphous solids. High resolution instruments operating at KIT-INE (liquids) and JRC-ITU (solids) offer the opportunity to apply this technique to actinide containing materials through the FP7 trans-national access programme EURACT-NMR (www.euract-nmr.eu).

- Underlying mechanistic models are conceptualisations of fission gas generation and transport within the fuel. For UO_2 fuel characterised by high burn-up, the following processes are typically considered (Blair, 2008):
    - Gas generation due to the fission of ^{235}U.
    - Recoil and knock-out.
    - Lattice (intra-granular) diffusion.
    - Grain-boundary diffusion.
    - Trapping (intra- and inter-granular)
    - Irradiation-induced resolution.
    - Intra-granular bubble motion.
    - Grain growth.
    - Grain boundary bubble development.

The adequate modelling of the fission gas generation and release requires considering a number of mutually interdependent processes (described above). A more detailed description of how these processes can be represented mathematically is given in Blair (2008), Van Uffelen (2002) and Pastore (2012).

5. Investigations on fast/instant release and contributions of the CP project

The project was organised into 4 different technical work packages:

- WP1. Samples and tools: Selection, characterization and preparation of materials and set-up tools
- WP2. Gas release + Rim and grain boundary diffusion: Experimental determination of fission gases release. Rim and grain boundary diffusion experiments
- WP3. Dissolution Based Release: Dissolution based fast radionuclide release
- WP4. Modelling: Modelling of migration/retention processes of fission products in the spent fuel structure

In this section, a review of the contributions of the project in each one of the subjects developed is highlighted. Detailed information on experimental techniques, characterization, experiments and models developed can be found in the reports of the project and in the 3 annual workshop proceedings.

Materials selected under study within CP FIRST-Nuclides

A complete description of the fuels used in the experimental programme is summarised in the. Final Scientific Report of the project (Deliverable D.5.13) as well as in the deliverable D1.2 and will not be repeated here (available at the project website: www.firstnuclides.eu).

Table 2 shows that selected materials fit into the range of present high burn-up fuels which need to be disposed of in Europe. Some non-standard materials are included, such as a fuel produced by a low temperature sintering process (NIKUSI), a fuel having Al and Cr additions and one high burn-up fuel kept for 14 cycles in a reactor. The other types of materials cover irradiated and unirradiated TRISO particles and the determination of the activity release from damaged and leaking VVER fuel rods.

Table 2. Characteristic data of fuel under investigation in CP FIRST-Nuclides.

		PWR	**BWR**	**THTR / VVER**
Discharge Manufacturer		1989 -2008 AREVA	2005 – 2008 AREVA/Westinghouse	
Cladding	**Material**	Zry-4 – M5	Zry-2	Graphite / Zr1%Nb
	Diameter	9.50 - 10.75 mm	9.84 - 10.2 mm	
	Thickness	0.62 - 0.73 mm		
Pellet	**Enrichment**	3.80 – 4.94 %	3.30 -4.25 %	2.4 -16.8%

	Grain size **Density** **Specifics**	5-40 µm 10.41 g cm^{-3} standard, NIKUSI production	$6 \leq x \leq 25$ µm 10.52 g cm^{-3} standard and Al/Cr addition to UO_2	20 -80 µm 10.8 g cm^{-3}
Irradiation	**Burn-up** **Nº cycles**	50.4 – 70.2 GWd/tHM 2 - 14	48.3 – 57.5 GWd/tHM 5 – 7	
Linear power	**average**	186 -330 W/cm	160 W/cm	130 – 228 W/cm
FGR		4.9 – 23 %	1.2 – 3.1 %	

It can be seen that the spent nuclear fuel considered in the CP FIRST-Nuclides consists mainly of high burn-up UO_2 fuel, and one MOX fuel, irradiated in commercial nuclear power reactors, and there is one group which studied the TRISO fuel, irradiated in a research reactor at Petten JRC. Also one VVER fuel rod, stored in water for several years has been investigated.

The ***PWR*** fuel burn-up of the samples used in the project ranged between 50 and 71 GWd/t_{HM}, with initial enrichments in ^{235}U of 2.8 to 4.3% and a PWR MOX fuel with a burn-up of 63 GWd/t_{HM} and initial Pu enrichment of 5.5%. FGR determined by Kr and Xe analyses by fuel rod puncturing rendered values between 5% and 27%.

In the case of ***BWR*** samples, the burn-up ranged from 42 to 60 GWd/t_{HM}, with ^{235}U enrichments between 3.7 and 4.3%, and determined FGR between 1% and 4%.

An interesting observation from the PWR samples is that the values of the FGR do not correlate well with the burn-up of the sample, but with the linear heat rate, as can be seen in Figure 8.

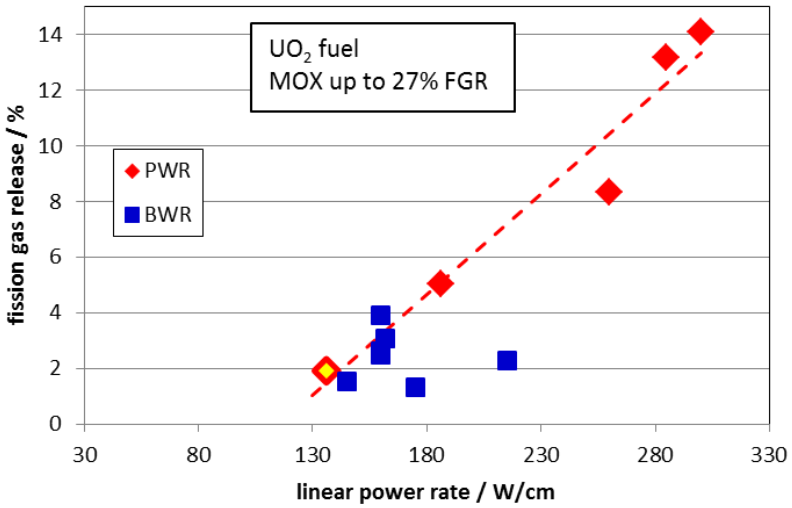

Figure 8. Variation of FGR versus Linear power rate for the materiasl investigated in the project.

One of the lessons learnt from the project is the relevance of compiling irradiation history of the fuel as well as some other properties of the material. The FGR values may depend on manufacturing process, temperature history, storage time, etc. It is thus essential to compile critical parameters, as done in the project (see D1.2 for details) to intepret some of the results obtained.

The project provided many data on characterisation of the selected samples, in some cases by developing new methodologies and tools.

Techniques such as non-destructive analyses of the fuel rods, scanning and defect identification of the cladding, technologies to cut and declad the fuel samples, post irradiation determination and quantitative determination of the inventory of the fuel samples by complete digestion of the fuel rod fragments and by laser ablation mass spectrometry were developed. Speciation analyses by using μ-scale synchrotron techniques were also applied.

A picture of the cutting process of cladded segments at ITU is shown in Figure 9.

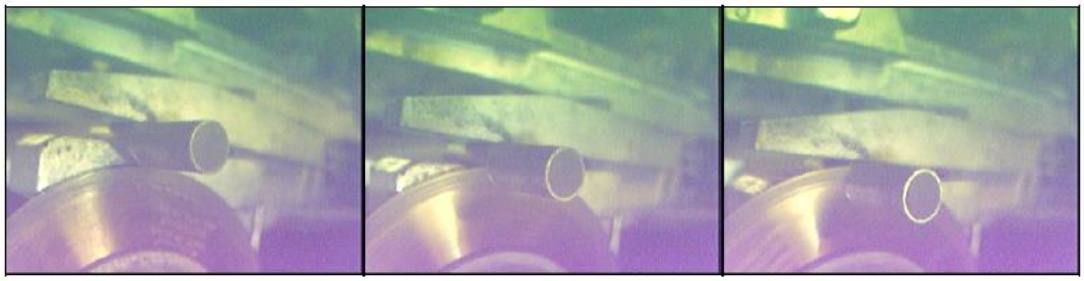

Figure 9. Cutting of cladded segments at ITU (BWR54 sample)

Gas release + Rim and grain boundary diffusion

Determination of FGR was done by different approaches:

- Puncturing of the plenum of a SNF segment of the Gösgen reactor was conducted and analysed for Xe and Kr at INE. The FGR was calculated for the experimental determination and the ORIGEN code was used to calculate the total fission gas inventory (González-Robles et al., 2013). The results indicated a FGR of means of 8.35% for Xe+Kr.
- Knudsen cell coupled to a mass spectrometer. JRC-ITU examined the release of the fission products ^{88}Sr, ^{87}Rb, ^{137}Cs, and ^{136}Xe from powder of irradiated BWR UO_2 (54 GWd/t_{HM}) originating from the core region of the fuel pin. The sample was heated in a Knudsen cell coupled to a mass spectrometer under vacuum conditions at a rate of 10 K/min until complete vaporization of the fuel at 2,460 K. The measured release profiles indicated two release mechanisms for ^{137}Cs, one with rather low intensity starting just below 1,000 K and a second significant release after 1,500 K. The release

of the fission products ^{88}Sr, ^{87}Rb, ^{137}Cs, and ^{136}Xe has been semi-quantified (Colle et al., 2014).

- The radial fission gas and volatile fission product distribution (Xe, I, and Cs) was analysed by Laser-Ablation Mass Spectroscopy (LA-MS) on HBU boiling water reactor (BWR) SNF (Wegen et al. 2014, Roth et al., 2013; Puranen et al., 2013). The technique provided very promising results, showing the radial distribution of the different elements (see Figure 10).

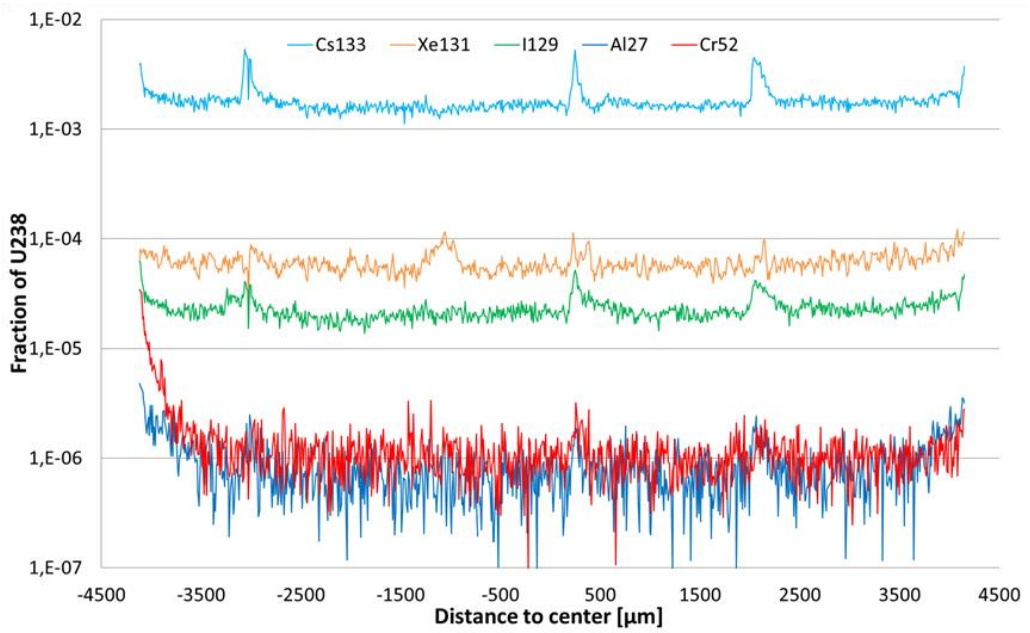

Figure 10. Ablation profiles on 5A2 (from Roth et al., 2013).

Rim and grain boundary diffusion

Diffusion of oxygen in spent UO_2 fuel can help quantifying the penetration of water in the fuel structures, and thereof can be relevant for the corrosion phenomena. Diffusion of oxygen and water penetration into UO_2 under both oxidising and reducing conditions has been studied by ITU, reproducing the range of concentrations expected when oxygen will be formed through α and β-radiolysis.

Under oxidising conditions and in presence of carbonate, the main part the UO2 surface is oxidised and reacts with carbonate which then forms a carbonate layer on the surface. Modelling of the resulting 18O penetration curve, under oxidative conditions, can only be explained by two parallel 18O diffusion processes. The first process was assigned to the lattice diffusion of oxygen in UO_{2+x}, with $x<0.25$ (limiting phase is U_4O_9). The second process indicate a significant grain boundary diffusion contribution. The modelling results are supported by alternated SIMS depth profiling and ion mapping showing local crater areas with significantly varying ^{18}O concentrations.

Dissolution based fast radionuclide release

Different groups have generated dissolution data on spent nuclear fuel during the project. All data generated is gathered in the database compiled during the project, together with data obtained from investigations previous to the FIRST-Nuclides project.

In order to assess the advances produced by the investigations, in the following subsection a summary of the results previous to the project is given.

Investigations previous to the FIRST-Nuclides project

In this section, previous investigations on fast/instant release are summarised. The data generated after 2005 uses Johnson's et al. definition on the fast/instant release (Johnson et al., 2012). Since SKB 91, the Spent Nuclear Fuel (SNF) source term in a water- saturated medium is described as the combination of two terms:

1. A fraction of the inventory of radionuclides that may be rapidly released from the fuel and fuel assembly materials at the time of canister breaching. In the context of safety analysis, the time of mobilization of this fraction can be considered as an instantaneous release of some radionuclides at the containment failure time.
2. A slower long-term contribution corresponding to the dissolution of the uranium oxide matrix, induced by α-radiolytical oxidation processes and impeded by the effect of hydrogen. The so-called hydrogen effect, which reduces the matrix dissolution extent, has been incorporated in a later stage.

In 2005, Johnson et al. generated a number of tables covering the fast release (leaching) data gathered until 2005. In the following, the different leaching experiments with SNF (UO_2 and MOX) that have been performed during the last 30 years are summarised. In some cases, although the work was not focused on the study of the IRF, it is possible to calculate it. The experiments were carried out using, essentially, four type of samples:

- Bare fuel: consisting of a piece of fuel and cladding with an artificially produced defect.
- Pellet: this term will be used when referring to a cladded fuel segment.
- Fragments: pieces or portions of fuel without cladding.
- Powder: fuel material obtained after de-cladding, sieving and milling.

❖ The earlier IRF data was generated within the US Yucca Mountain project. The publications cover the span: 1987 to 1990; Oversby and Shawn (1987); Wilson, 1987; Wilson and Shawn (1987); Wilson (1988); Wilson, (1990 a, b); Wilson and Gray (1990). In this work they used two bare fuel specimens prepared from, HBR-type fuel (BU of 30 GWd/t_{HM}) and TP-type fuel (BU of 27 GWd/t_{HM}) PWR SNF's. The tests were conducted

in unsealed silica vessels under ambient hot cell air and temperature conditions. The initial weight was 83.10 g for HBR SNF and 27.21 g for TP SNF. The leaching solution was J-13 water, which corresponds to the chemical composition of the J-13 well in Yucca Mountain. The composition in mmol/L was: Na^+ 2.2; K^+ 0.13; Ca^{2+} 0.38; Mg^{2+} 0.08; Si 1.14; F^- 0.37; NO_3^- 0.15; SO_4^{2-} 0.2; HCO_3^- 2.0, pH 7.2. Two leaching cycles were performed consecutively. The experiments were carried at 25 and 85°C. The data reported in Table 1 correspond to the sum of the two cycles that means a total leaching time of 425 days for HBR SNF and 376 days for TP SNF.

- Within the Yucca Mountain project additional IRF dissolution tests were performed; Gray and Wilson, (1995) Gray (1998): measured the gap and grain boundaries inventories from different PWR SNF's: ATM-103 (BU of 30 GWd/t_{HM}), ATM-104 (BU of 44 GWd/t_{HM}) and ATM-106 (BU of 43 and 46 GWd/t_{HM}), and from BWR SNF's: ATM-105 (BU of 31 and 34 GWd/t_{HM}).

  The fuel specimens were prepared from 12 to 25 mm long SNF-segments. To measure the gap inventories, the SNF was discharged from the cladding and placed in a glass vessel along with the empty cladding segment. A measured volume (200 to 250 mL) of distilled ionised water (DIW) was added to the vessel and allowed to stand for 1 week at hot cell temperature under ambient atmosphere. Grain boundary inventory measurements were performed on the SNF specimens after completion of the gap inventory measurements. After one week exposure to water, the SNF fragments were dried, crushed, and screened using screens with 20 to 30 µm openings, depending on the grain size of the SNF being prepared. The grain-boundary inventory measurements consisted of placing 0.5 g of the screened SNF grains and subgrains in a 50 mL beaker along with 20 mL of 0.1 M HCl. Periodically after 3 h the acid was removed, filtered, and replaced with fresh acid.

- The Swedish program performed characterization of fuel samples and dissolution experiments of a number of specimens from the Oskarsham and Ringhals reactors. Forsyth and Werme (1992); Forsyth (1997): experiments performed with 20 mm long fuel/clad segments from Oskarsham-1 BWR SNF (BU of 42 GWd/t_{HM}), Rignhals-1 BWR SNF (BU between 27.0 and 48.8 GWd/t_{HM}), and from Rignhals-1 PWR SNF (BU of 43 GWd/t_{HM}). The specimen, a fuel/clad segment suspended in a spiral of platinum wire, was immersed in 200 ml of the leaching solution in a 250 ml Pyrex flask. All tests were performed at 20-25°C, ambient temperature of the hot cell and under oxidizing conditions. The solution compositions used were DIW (De-Ionized water) and GW (GroundWater), the composition in mmol/L of the GW used was: Na^+ 2.8; K^+ 0.1; Mg^{2+} 0.2; Ca^{2+} 0.45; Si 0.2 HCO_3^- 2.0, Cl^- 2.0; SO_4^{2-} 0.1. The experiments were performed at room temperature and contact times were of the order of 7 days.

- Within the Spanish programme, Serrano et al. (1998) conducted experiments with irradiated fuel samples prepared from pins of two SNF's: UO_2 (BU of 54 GWd/t_{HM}) and MOX (BU of 30 GWd/t_{HM}). Sequential batch leaching experiments in DIW at room temperature under ambient atmosphere were made. On completion of the selected contact period, the samples were transferred to clean vessels containing fresh solution. The leaching times encompassed an interval between 24 and 1300 hours. The vessels were, after used, rinsed with 1M HNO_3 for 1hour at room temperature. During the experiment, the vessels were kept closed tight; after the longest leaching time, no significant loss of leachate from the bottles was observed. The leaching experiments with irradiated fuel were performed in a hot cell at an ambient hot cell temperature of 25±2 °C.

- IRF characterization and dissolution data generated in the Transuranium Institute was reported by Glatz et al., 1999. In this work, three MOX SNF´s (BU of 12, 20 and 25 GWd/t_{HM}) and three UO_2 SNF´s (one with 30 GWd/t_{HM} and two with 50 GWd/t_{HM}) rods, each of them about 6 cm long were used. Both ends of each rodlets were closed by means of tight stainless steel end-caps. One UO_2 fuel rod with a burn-up of 50 GWd/t_{HM} was machined to produce two defects (in each case, 3 holes of 1 mm diameter each), one at the top and in contact with vapour and the other at the bottom of the rod and in contact with the leaching solution. In all the other samples, the defects were placed in the centre of the rod and the autoclave was filled completely with the leaching solution. MOX fuels were fabricated following the MIMAS blend process. The leaching experiments were carried out in autoclaves equipped with Ti-liners, using DIW at 100°C under anoxic or reducing conditions.

- The German programme reports work on spent fuel dissolution since the early 90's. Loida et al. (1999) reported ^{137}Cs the initial release of ^{137}Cs from various spent fuel materials measured in $MgCl_2$-rich and concentrated NaCl solutions at 25, 90, 100, 150 and 200°C. These experiments cover mainly fuels of a burn-up between 36 and 50 GWd/t_{HM}. Most of the ^{137}Cs IRF are below or in the range of the pessimistic values compiled by Poinssot and Gras (2009). An IRF of 3.7% of the total ^{137}Cs was measured in a leaching experiment with a spent nuclear fuel sample from the NPP Biblis (KWB, discharged June 1979; burn-up of 36.6 GWd/t_{HM}) in concentrated NaCl solution at 200°C. This value is slightly higher than the pessimistic ^{137}Cs IRF estimate for fuel with a burn-up of 41 GWd/t_{HM}. The experiments were performed partly at FZK (today KIT) and partly at KWU.

- In a later stage of the Spanish programme, Quiñones et al., (2006): investigated three UO_2 PWR SNF's samples: U-568 (BU of 29.5 GWd/t_{HM}), B4 (BU of 53.1 GWd/t_{HM}) and AF-02 (BU of 62.8 GWd/t_{HM}). Discs containing cladding and fuel with an approximately thickness of 2 mm were cut from the fuel rods. The weight of the SNF contained in these discs was about 2 g. Two samples of each specimen were prepared. Static batch leaching

experiments were performed in 70 mL volume borosilicate glass vessels. All experiments were performed at room temperature, in a hot cell with air atmosphere. The leaching solution consisted of 50 ml of simulated groundwater, of the following composition (in mol/kg_{H2O}): Na^{+} $4.09\cdot10^{-4}$; K^{+} $1.46\cdot10^{-4}$; Mg^{2+} $2.51\cdot10^{-4}$; Ca^{2+} $2.47\cdot10^{-4}$; Cl^{-} $2.37\cdot10^{-4}$; Si $4.99\cdot10^{-4}$; SO_4^{2-} $7.19\cdot10^{-5}$; HCO_3^{-} $1.07\cdot10^{-3}$; F^{-} $1.05\cdot10^{-5}$; PO_4^{3-} $1.04\cdot10^{-7}$; Al^{3+} $1.85\cdot10^{-7}$; U_{total} $2.32\cdot10^{-9}$; pH around 7.0. The solution was de-aerated by purging it with inert gas for several hours prior to the start of the leaching. During each contact period, the vessels remained sealed.

- Although spent fuel is not a priority in the French waste management program, there has been substantial work performed by the CEA groups with respect to IRF characterization and dissolution. Roudil et al. (2007), Roudil et al. (2009): investigated five PWR SNF's samples, four UOX with a BU of 22, 37, 47 and 60 GWd/t_{HM}; one MOX with a BU of 40 GWd/t_{HM}. Two types of samples were used: i) 20 mm segments with cladding and ii) powder samples with a particle size of 20-50 µm. Powder samples were only prepared for the 60 GWd/t_{HM} BU SNF. The experiments were carried out under oxidizing conditions at room temperature (25 °C).

The gap inventories were determined by static mode leaching experiments in carbonate water (10^{-3} M HCO_3^{-}) with 20 mm clad segments of the five SNF´s. The tests, under air atmosphere, lasted for 62 days with leachates sampled at the following intervals: 3, 10, 24 and 62 days.

Experiments to determine the inventory at the grain boundaries were carried out only on UOX PWR fuel with a BU of 60 GWd/t_{HM}. Leaching experiments were carried out on SNF powder according to a protocol similar to the one developed and validated by Gray and Wilson (1995).

SNF fragments were sampled from the centre of a clad 35 mm segment previously leached for one week in carbonated water to eliminate the gap inventory. Sampling the fragments at the centre of the segment also eliminated the contribution of the rim. Powder samples with a particle size fraction of 20–50 µm were therefore prepared by grinding and sieving in a hot cell. The number of grains in each particle was estimated to be about forty.

Pseudo-dynamic leach tests, under air atmosphere in hot cell, were carried out on 567 mg of powder in 25 mL of carbonated water (10^{-2} M $NaHCO_3$) to prevent any precipitation of uranium used as a matrix alteration tracer. After each cycle the solutions were filtered and analysed. Fresh water was added to the leaching reactors. Thirty cycles were carried out, initially of short duration (1–2 h) to avoid any precipitation resulting from leaching of the oxidized UO_{2+x} layer, then longer (24–48 h). When the ratio of the released fractions was equal to 1 it was assumed that the complete inventory at the grain boundaries was leached during the preceding cycles.

Roudil et al., 2009: also studied the IRF coming from fragments and grains from the pellet peripheral zone coupon, near or in contact with the cladding. They used a PWR SNF´s with a BU of 60 GWd/t_{HM}.

Each fuel segment was first slotted to obtain two cylindrical portions separated from the core and consisting of cladding and peripheral fuel. The cladding was then separated from the fuel with a mortar and pestle. The resulting fragments were separated by sieving using 20 and 50 microns screens. To increase the proportion of small grains, such as those in the rim, the powder used for the leaching experiments was sampled from the particle size fraction below 20 microns.

The leach tests were carried out on 282 mg of powder in about 25ml of bicarbonate water to prevent any precipitation of uranium used as a matrix alteration tracer. After each cycle a solution sample of about 17 mL was removed to avoid carrying away powder, filtered to contact with the fuel powder for the next cycle. Twenty cycles were performed in all. The initial cycles were shorter (lasting only few hours) to avoid uranium precipitation due to leaching of the oxidized UO_{2+x} layer. The subsequent cycles lasted 24 hours each.

- Within the Korean waste management programme, Kim et al. (2007) measured gap and grain boundaries in three different PWR fuel rods: SFR1 (BU of 39.6 GWd/t_{HM}), SFR2 (BU of 39.6 GWd/t_{HM}), SFR3-a (BU of 45.8 GWd/t_{HM}) and SFR3-b (BU of 65.9 GWd/t_{HM}). The fuel specimens were prepared by cutting fuels rods thereby obtaining discs with 2 mm thickness.

  The gap inventory was measured on a SNF pellet without cladding. The SNF and cladding were put into a bottle filled with 100 ml of distilled water. The experiment was run under hot cell conditions. Subsamples consisting of 5 ml of the leachate were sampled after leaching time intervals longer than 7 days.

  Two types of SNF powder, sawdust produced during the cutting of fuel rod SFR1 and crushed powder produced by crushing the specimens after the gap inventory experiment, were used for a measurement of the radionuclide inventories in the grain boundaries. In the case of the sawdust, the inventory of the nuclides in the grain boundaries was calculated from the IRF, which is the combined inventories of the gap and the grain boundaries. The powder was leached in 50 ml of 0.1M HCl for about 20 minutes and the solution was sampled by filtering it through a 0.2 μm filter. The solution was replaced with a fresh acid and subsequently sampled.

❖ Within the Swedish programme, Fors, 2009; Fors et al., 2009. A commercial UO_2 SNF with a BU of 59.1 GWd/t_{HM} and an average power line of 250kW/m was used.

A 10 mm long segment was cut from a position of the fuel rod. The segment was core drilled to separate the fuel centre from its peripheral 725 μm thick rim part. The fuel containing the high burn-up structure (HBS) material was detached from the Zircaloy cladding by use of external stress in a screw clamp. The de-cladded fuel fragments contained about 15 wt.% HBS. The millimetre-sized fragments were stored under dry N_2 atmosphere (<2 vol.% O_2) for one year before the start of the corrosion experiment. The leachant contained 10 mM NaCl and 2 mM $NaHCO_3$. The pH of the initial solution was 8.1. After the leachant filling, the autoclave was pressurized to 4.1 MPa with hydrogen. This pressure was kept throughout the experiment. The experiment was carried out at ambient hot cell temperature at 23 ± 4°C. The leachate was not stirred.

❖ Recently within the Swedish programme, Johnson et al. (2012): published two works performed at Studsvik and Paul Scherrer Institute (PSI).

The work at Studsvik consisted of four commercials UO_2 SNF´s: Ringhals 3 (PWR, BU of 58.2 GWd/t_{HM}), Ringhals 4 (PWR, BU of 61.4 GWd/t_{HM}, Ringhals 3 (PWR, BU of 66.5 GWd/t_{HM} and North Anna (PWR at North Anna NPP in Virginia, USA, BU of 75.4 GWd/t_{HM}).

Two samples were cut from near the middle of each of the four fuel rods. A fuel corrosion sample consisting of a 20 mm segment was cut at mid-pellet height and contained one complete and two half pellets. These samples are referred to as closed rod samples. In another set of tests, referred to as open rod samples, adjacent fuel rod segments of 20 mm length were cut from each of the four rods and were weighed. The cladding was carefully sawn on both sides of the segment periphery and force was applied to the halves until the fuel broke away from the cladding. The two cladding halves, together with detached fuel fragments were collected in a glass vessel with glass filter bottom (100–160 μm pores) and weighed again. Then they were leached according to the same procedure as the closed rod samples. An initial solution sampling 2 h after test start was also carried out for all samples of this test series. The samples, kept in position by a platinum wire spiral, were exposed to 200 ml of synthetic Allard groundwater in a Pyrex flask. The pH was stable around 8.3 and carbonate concentration remained constant during all the experiments. The composition of the Allard water in mmol/L was: 0.45 Ca^{+}, 0.18 Mg^{+}, 0.1 K^{+}, 2.84 Na^{+}, 0.21 Si, 2.01 HCO_3^{-}, 0.1 SO_4^{2-}, 1.97 Cl^{-}, 0.2 F^{-}, 0.001 PO_4^{-}. The contact periods were 2 h, 7, 21 and 63 days. More information about these experiments can be found in Johson et al., 2012.

The PSI work consisted of three commercial SNF specimens: Leibstadt (BWR, UO_2 BU of 65.3 GWd/t_{HM}) Gösgen (PWR, UO_2 BU of 64 GWd/t_{HM}), Gösgen (PWR, MOX BU of 63 GWd/t_{HM}). The length of the fuel rod segments was 20 mm (two pellets) for each leaching experiments. For the rim samples the inner part of the fuel was removed mechanically by

drilling (unintentionally somewhat off-center), leaving an asymmetric ring of fuel bonded to the cladding. One rim sample was left open, whereas a tight-fitting PVC plug was placed through the entire length of the other rim sample. In order to investigate if the fuel surface available for the attack of the leachant had a significant impact on the leach rate, a number of samples were broken into two halves, by cutting the cladding on opposite sides. Glass columns (total volume approx. 250 mL) with a sealed outlet tap for sampling and an implemented glass filter in order to retain solid particles were used. Approximately 200 ml of buffer solution (28 mM borate buffer, pH 8.5, containing 20 µg/g NaI as iodine carrier) were used per sample for the leaching experiments. As the objective of the measurements was to obtain the rapid release fraction of certain radionuclides, the experiments were performed in air-saturated buffer solutions. After filling the columns with the sample and buffer solution the supernatant air volume was removed through a hole in the piston cylinder which was closed afterwards to avoid additional air intake. Subsamples of 20 mL each were taken after 7, 14, 21, 28 and 56 days, whereas the last sampling of 30 mL per leach solution was performed after 98 days.

- Also within the Spanish programme, Clarens et al. (2009), González-Robles (2011), Serrano-Purroy et al. (2012): used four commercial UO_2 SNF´s: three from PWR with a BU of 48, 52, 60, GWd/t_{HM} and one from a BWR with a BU of 53 GWd/t_{HM}. The temperature was (24 ± 6)°C.

  From the SNF´s with a BU of 48 and 60MWd/kgU, three different SNF samples corresponding to the central axial position (labelled CORE), the periphery of the SNF pellet (labelled OUT) and to an emptied cladding segment with small amounts of SNF attached to the inner wall called CLAD were prepared. In order to remove fines attached to the grain surface, the CORE and OUT powder SNF fractions were washed several times with acetone.

  Static leaching experiments of powder samples, CORE, OUT and CLAD, were carried out in (50 ± 0.1) mL borosilicate glass test tubes with dimensions of length of 150 mm and a diameter of 25 mm with thread and a plastic screw cap (Schütt Labortechnik GmbH, Göttingen, Germany). The tubes were placed on a rotating stirrer (nominal speed of 30 rpm) to avoid concentration gradients that could influence the dissolution rate. Static leaching experiments were carried out with two synthetic leaching solutions: bicarbonate (BIC), which composition in mM was: 19 Cl^-; 20 Na^+; 1 HCO_3^-, pH 7.4; and Bentonitic Granitic Groundwater (BGW), with following composition in mM: Cl^- 93.9; SO_4^{2-}45.2; HCO_3^- 0.9; Na^+ 117.9; K^+ 1.1; Ca^{2+} 15.4; Mg^{2+} 17.3; pH of 7.6. The experiments were carried out under oxidising conditions and with about 0.25 g of SNF (Clarens et al., 2009; González-Robles et al., 2011; Serrano-Purroy et al., 2012).

Static experiments of pellet samples of the four SNF´s were performed in a (50 ± 0.1) mL flask and daily shaken for 5 to 10 minutes to avoid the risk of breaking the flask through the manual shaking.

The head space of the gas phase was (3 ± 1) mL for the powder sample experiments and (10 ± 1) mL for the pellet samples. To avoid initial U saturation and secondary phase formation, the solution was completely replenished two times at the beginning of each experiment.

Selected values from the reporting results are shown in Figure 11 and Figure 12. The data shown are selected taking into account the experimental conditions such as sample preparation, aqueous phase, the use of pellets, fragments or powders, etc.

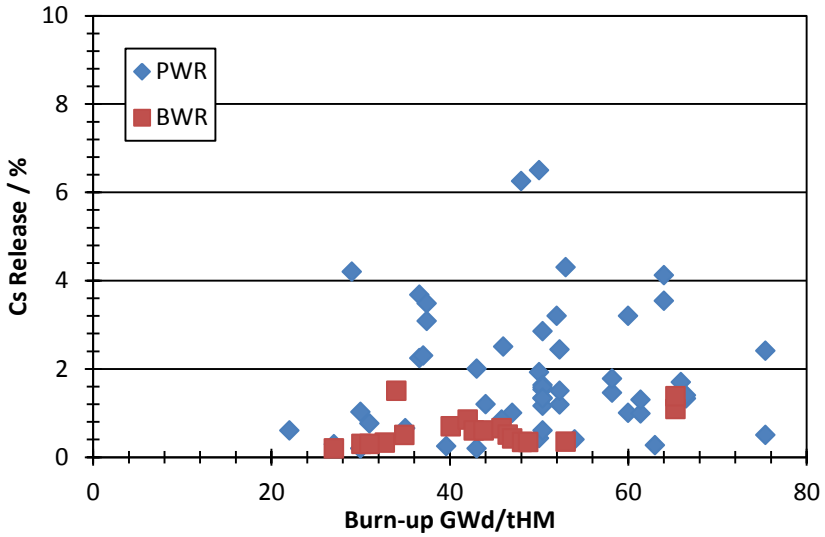

Figure 11. Fast Cs release as function of burn-up.

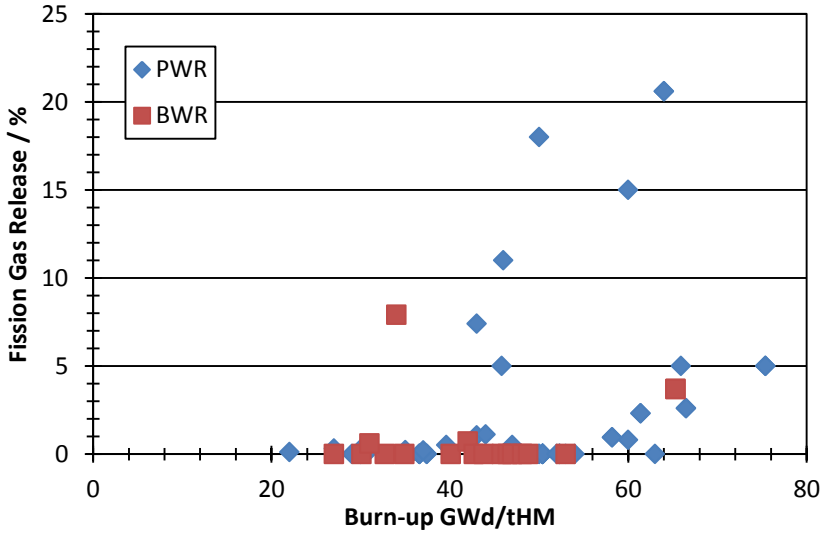

Figure 12. Fission gas release as function of burn-up.

Figure 11 shows the Cs release and Figure 12 the fission gas release as function of burn-up for PWR and BWR fuels. FRG or Cs release of zero means that these data are not given in the related publications. Most of the experiments were performed with fuel having a burn-up below 50 GWd/t_{HM}. In almost all cases, the Cs release is below 5%, only two measurements (not shown) reveal significantly higher values.

In total, the data show some scatter and especially in Figure 12 two trends can be observed: one increasing at 40 GWd/t_{HM} and another at 60 GWd/t_{HM}. If only results where both type of data, FGR and Cs, are considered, a different picture appears (Figure 13), from where a linear correlation between Cs release and FGR is observed.

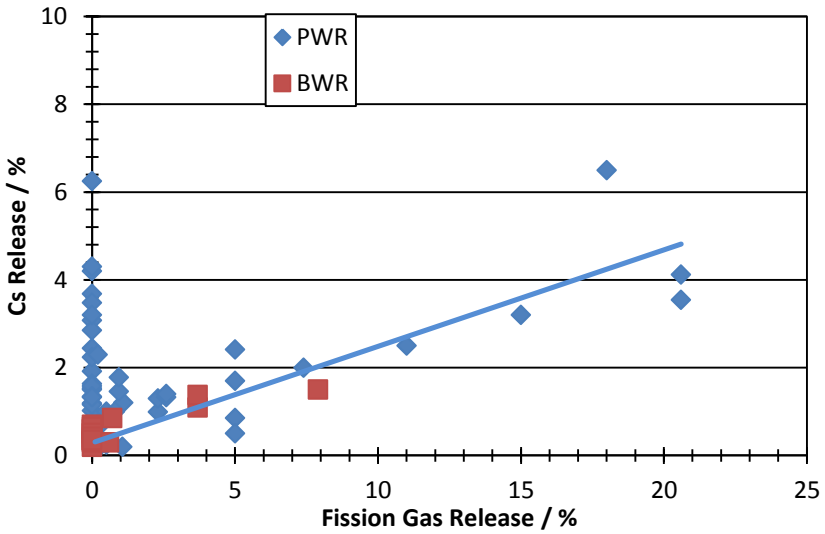

Figure 13. Cs release as function of the fission gas release.

Variations in FGR and correlations with FP release can be important depending on the irradiation history of the fuel, the sample preparation and the leaching conditions, what makes difficult to extract generalized numbers accounting for IRF. What is clear is that complete information on burn-up and linear power rate, temperature reached, and evolution of the porosity of the fuel during the irradiation stages are important, among other factors, to derive reliable correlations and to understand apparent variations in the SF IRF and FGR behaviour.

Investigations conducted in the FIRST-Nuclides project

The experimental investigations include the release of gaseous and non-gaseous fission products from high burn-up UO_2 fuel (~ 60 GWd/t_{HM}) and establishing correlations between the fission gas release (FGR) and the release of non-gaseous fission products. A recent study by Johnson et al. (2012) demonstrates the importance of the linear power on the FGR. For this reason, it is beneficial for the project to investigate SF from different reactors and different operation strategies, such as the number of irradiation cycles.

The investigations aim at reducing uncertainties with respect to ^{129}I, 135Cs, ^{79}Se and ^{14}C release and speciation, and will provide for improved data for these isotopes. The chemical form of the relevant elements requires also specific investigations, as the migration and retention behaviour depends strongly on their cationic or anionic character.

6 groups conducted dissolution-based investigations in FIRST-Nuclides: KIT-INE, SCK-CEN, PSI, Studsvik, ITU and CTM. The leach experiments by the various institutes were harmonized as much as possible to allow a better comparison of the leach data. For this reason, a standard leachant (19 mM NaCl and 1 mM $NaHCO_3$) was used by most laboratories, and tests with similarly prepared samples (cladded fuel segments) were added by several laboratories. Nevertheless, there were also differences in experimental approaches, such as the redox conditions (reducing or oxidizing atmosphere), leaching mode (static or pseudo-dynamic), and alternative sample preparations. Both PWR and BWR fuels were tested. One test series with a MOX fuel was also performed. Maximum duration time was of. Most laboratories measured the most critical IRF radionuclides, i.e. Cs and I isotopes. Other isotopes that were measured by several, but not all laboratories are ^{14}C and ^{79}Se. For some isotopes, the analytical methods were developed in the framework of the project. Special efforts were made to characterize selenium in the spent fuel by solid state analyses.

The radionuclides investigated by each group are shown in Table 3.

Table 3. Radionuclides analysed by each group in the dissolution-based experiments.

	^{14}C	Kr+Xe	^{79}Se	Rb	^{90}Sr	Mo	^{99}Tc	Pd	^{129}I	^{137}Cs	U	Pu
KIT		x			x		x		x	x	x	
ITU				x	x	x	x	x		x	x	
PSI									x	x		
SCK·CEN	x				x	x	x	x		x	x	x
CTM				x	x	x				x	x	
Studsvik			x		x	x	x		x	x	x	

It is also important to realize the difference in the solid samples, as shown in Figure 14.

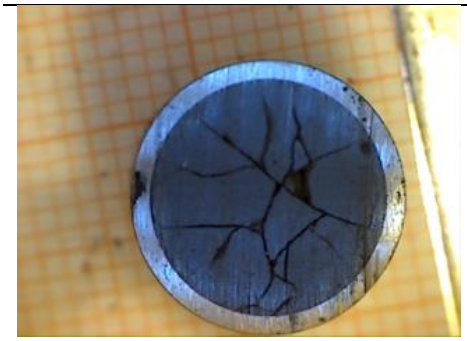

Picture of a cladded fuel segment used in the investigations

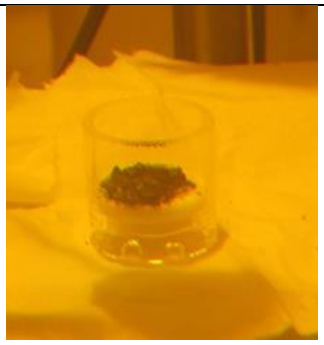

Image of mm-size fragments of fuel used in the investigations

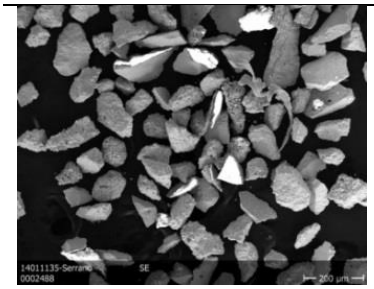

Powder used in some of the experiments, with particle sizes below 100 microns

Cladding plus adhered residues that have not been separated in the cutting and extraction process prior to the experimental tests.

Figure 14. Images of some of the different solid samples used in the investigations.

As well as the differences in the experimental conditions, as shown in Figure 15.

KIT: *-Standard leachant.* *Experiments in an autoclave with Ar/H_2 atmosphere:* ***-Reducing conditions.***	***ITU and CTM:*** *-Standard leachant.* *Cladded segments suspended in the solution.* ***-Oxidizing conditions**: calculation of the IRF must consider the substraction of FIAP of U dissolution.*	***Studsvik:*** *-10 mM NaCl+2 mM $NaHCO_3$* *Samples in a glass basket immersed in air saturated leaching solution.* *- **Oxidising conditions**: correction for UO_2 matrix dissolution needed before reporting IRF for other nuclides*
	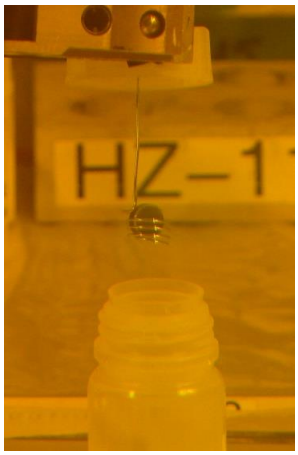	

PSI and SCK-CEN
-Standard leachant
-"pseudo-anoxic" conditions.
The piston minimizes the intrusion of O_2 from the hot cell, although there can be a small amount of UO_2 matrix dissolution

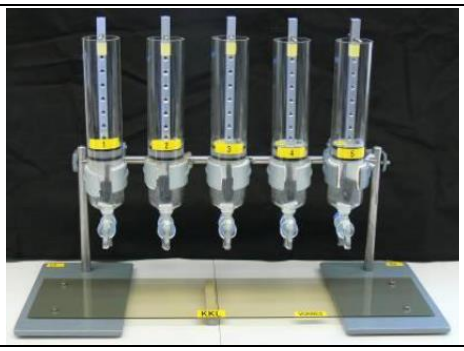

Figure 15. Different experimental set-ups used in the investigations by the different laboratories.

The results are detailed in the different contributions by each group: Curti et al. (2014a, b); González-Robles et al. (2014); Martínez-Torrents et al. (2014); Mennecart et al. (2014); Puranen et al. (2014b); Roth et al. (2014b); Serrano-Purroy et al. (2014); and the work on dissolution of the damaged VVER, which is reported in detail in Slonszki and Hózer (2014). The data generated has been included in the database of the project (Valls et al., 2014).

One of the findings supported by the experiments performed in the project was that FGR and other IRF was not well correlated with burn-up. The results obtained from the project are plotted together with existing data in the literature in Figure 16.

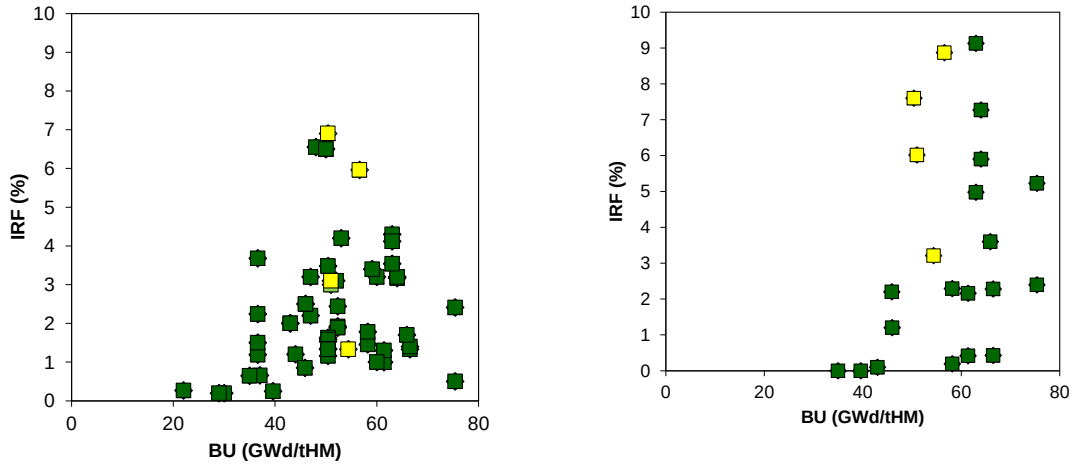

Figure 16. Data o f IRF of Cs and I versus burn-up for PWR fuel plotted as a function of burn-up. Left Cs(%); right I(%). Data previously existing in the literature are shown with dark markers and data generated within the project is shown with yellow symbols. It is clear that for the same burn-up, differences in the Cs and I IRFs can be important, showing the non-linear dependence of IRF with burn-up.

A very detail report on the individual findings has been done in the different annual workshop proceedings as well as in the final scientific report – D5.13 (Kienzler et al., 2014). A brief summary of the main findings obtained from dissolution based investigations is given below:

- Until recently, the IRF of spent fuel was often related to its burn-up. With more data becoming available for high burn-up fuel, there is growing evidence that the FGR and IRF depends much more on the linear power rating of the fuel than on the burn-up. The data gathered in FIRST-Nuclides give further convincing evidence for this. Hence, the linear power appears to be a more relevant operational parameter to predict the FGR than the burn-up is. This can be explained by the fact that the FGR depends on the temperature of the fuel pellet in the operator, while this temperature depends on the linear power, rather than on the burn-up.
- The measurements of the FGR during the leach test by KIT have shown that FGR takes place also during the leaching of the fuel. The amount of fission gases released in this way appears to be higher than the amount of fission gases released in the plenum during the fuel operation.
- The IRF values measured for Cs tend to be proportional to the FGR with a proportionality factor of 0.6. The IRF values measured for Iodine tend to be proportional to the FGR with a proportionality factor of 1. The difference between the Cs or Iodine release and FGR appears to increase in absolute terms with higher FGR, where the FGR increasingly overestimates the Cs or I release. To explain the increasing differences between Cs or I release and FGR at increasing FGR, a detailed analysis of each test should be performed. From the perspective of performance assessment, the upwards deviations (>0.6 x FGR for caesium, or >1 x FGR for Iodine) are more relevant than the downwards deviations. To include all measurement points, both from FIRST-Nuclides and from older experiments, an extra term corresponding to a caesium or Iodine release of about 2% should be added.
- The IRF of Cs or I determined from differently prepared samples (cladded segments, opened segments, fragments, powders…) are coherent. They depend on the exposed surface area and the nature of the exposed fuel structures (gap or grain boundaries). These data can be used further to estimate the relative contributions of the various fuel structures.
- The doping of UO_2 with Al/Cr appears to have a favorable effect on the IRF, which is probably due to the fact that the larger grain size increases the distance over which Cs and Iodine have to diffuse before they reach the grain boundary.
- The Cs dissolution rate decreases with time in the leach tests. The net dissolution rates measured for the damaged and leaking VVER fuel (after substraction of the UO_2 matrix dissolution rate) are of the same order of magnitude as the rates determined in the leaching tests, and also decrease with time. Nevertheless, in almost all leach experiments, a residual dissolution rate of Cs isotopes was measured between the longest test durations. This means that the measured IRF for the longest duration ≤ 1 year) may not be the long-term maximum. The net Cs dissolution rates measured in the leach tests were all significantly higher than the expected long term UO_2 matrix dissolution rate, even for the tests in reducing conditions by KIT. Extrapolation,

preferably supported by modeling, is necessary to estimate the time required for the complete release of IRF nuclides. The long-term matrix dissolution rate, and the time it will take before the release of IRF radionuclides is controlled by this matrix dissolution, will depend on the redox conditions. In reducing conditions, the matrix dissolution rate will be much lower than in oxidizing conditions. Moreover, matrix oxidation tends to open grain boundaries and thus causes the continuous exposure of fresh grain boundaries with high concentrations of soluble IRF nuclides.

- The IRF values measured in the leach tests can be compared with Performance Assessment oriented best estimate and pessimistic IRF estimations from a previous program (NF-PRO). It appears that Cs and I are confirmed as the most important IRF isotopes, and that the previous pessimistic estimates may underestimate the IRF of fuels that have undergone a high linear power rating. The new IRF data available for ^{14}C and Pd suggest that the previous estimations may be too pessimistic. The previous estimates for Sr and Tc are roughly confirmed by the new results. Se and Sn (left out as IRF nuclides in NF-PRO) may have small IRF contributions.

Modelling of migration/retention processes of fission products in the spent fuel structure

Modelling has been approached from different perspectives in the project:

1. Review of the different models available in the literature to describe FGR and couple with IRF data, as presented in more detail in section 3 of this report as well as in deliverable D4.1 of the project (Pekala et al., 2013)
2. Burn-up and decay history calculations performed using the webKorigen software package (Nucleonica, 2011)
3. Central temperature of a fuel rod under irradiation, rim zone thickness, the rim zone burn-up, and the Xe content and porosity of the rim zone. A model is presented which allows to calculate the temperature dependent diffusion and retention of volatile radionuclides within a fuel pellet during the irradiation period (Kienzler et al., 2014)
4. Kinetic model of radionuclide release
5. The development of the saturation model of a pellet immersed in water and the impact that this saturation can have on radionuclide release. Comparison with experimental data.

Kienzler et al. (2014) calculated the radial distribution of I and Cs in a spent fuel pellet by a temperature-dependent sorption parameter and show that the simulated concentration distributions correspond well to Studsvik's measurements by Laser Ablation Techniques. The temperature at the different zones of the rod has been calculated (see Figure 17) and the associated calculation of the volatile elements can be described by a temperature dependent

condensation process. After one year in the reactor, the calculated release of the volatile elements account to 1.3%, a number in the range of the fission gas release.

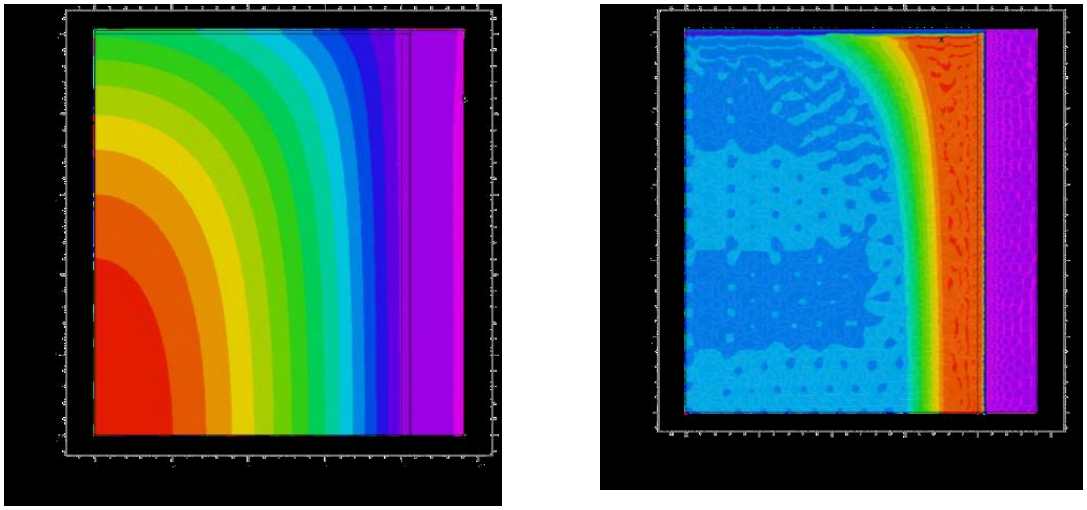

Figure 17. *Left*: Contour of the calculated temperature in the C1 rod (red: highest, magenta lowest; *Right*: Concentration distribution of the volatile elements in the pellet (red highest concentrations, blue: initial concentration, magenta: zero concentration).

Casas et al. (2014) present a kinetic model for the instant SF dissolution is developed as a sum of the contributions from different fuel phases. The dissolution of each different phase is considered as a first order kinetics, given by an equation of the type:

$$m_{RN}(t) = \sum_{i=1}^{N} m_{RN,i\infty} \cdot (1 - e^{-k_i \cdot t})$$

Where $m_{RN}(t)$ accounts for the total measured/predicted cumulative moles of the correspondent fission product released at a time *t*; $m_{RN,i\infty}$ which gives the total moles measured/predicted for the specified dissolving phase of the fission product and, k is the kinetic constant for the dissolution of that specific phase.

The models assume the homogeneity of the sample under study and also incorporate a fraction of matrix dissolution. 3 different components are defined: M1: very rapid initial dissolution from oxidized phases and/or fine particle; M2: the fraction of Cs that is being dissolved independently of U and M3: would be related to the matrix contribution. M2 is the contribution that would represent the Fast release fraction of Cs (see Figure 18)

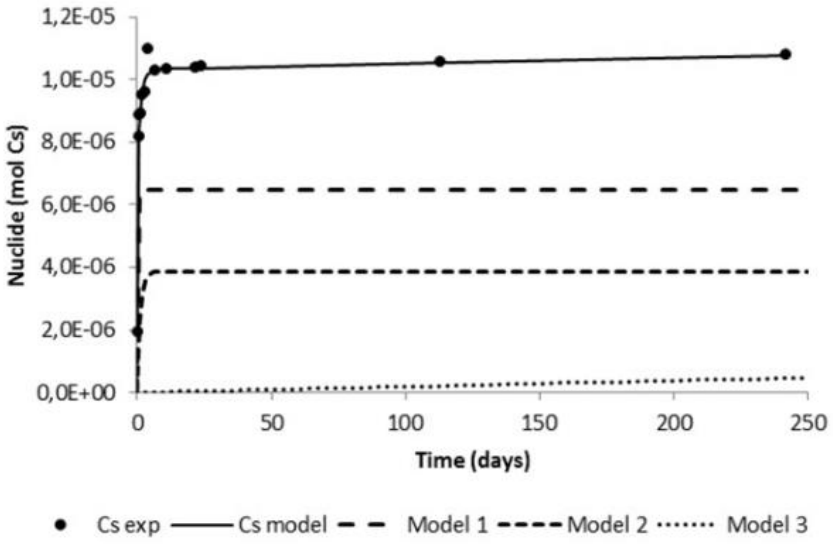

Figure 18. Comparison betwen experimental data on Cs release and the kinetic model developed and applied in the project.

The development of the model of saturation of the spent fuel pellet has been conducted and implemented in the finite element code *Comsol Multiphysics* using the Fracture Flow Interface (for flow in the "macro cracks") and the Richards Interface (for flow in the "micro cracks").with the aim to understand to which extent the water saturation may impact the fast release fractions. The model has shown interesting capabilities to couple with chemical retention processes of the radionuclides when releasing from the fuel. The details are given in Pekala et al. (2014) and the main results are summarised as follows:

1. Saturation of the "macro cracks" occurs rapidly, over a period of about 1 day. On the other hand, the saturation of "micro cracks" requires a much longer period of time (over 50 days).
2. 1D calculations of variably-saturated water flow (saturation) and diffusive-advective transport of a tracer from a single crack were performed in order to better understand the relative importance of flow and transport processes for the considered problem. Additional simulations were conducted for the complete interconnected network of "macro cracks". The fronts of water saturation and tracer concentration coincide closely. This is expected for a problem where water saturation constitutes a limiting factor for transport (see Figure 19)
3. Comparison with experimental data has shown that the initial release of fast nuclides from the fuel can be explained by considering the time needed for water saturation of the pellet (see Figure 19).

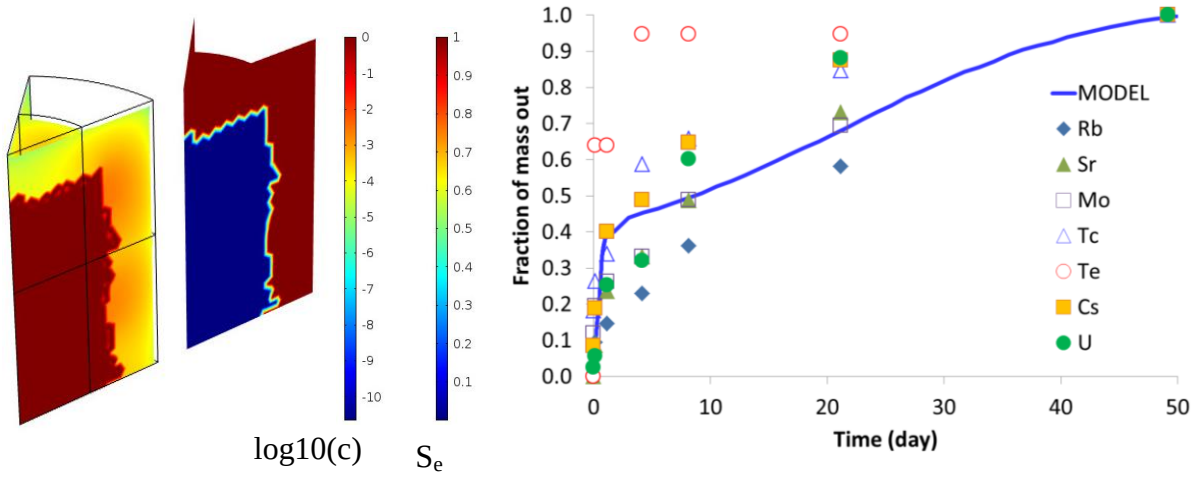

Figure 19. *Left:* Tracer concentration (log10[mol/L] – left) and saturation with water (S_e – right) calculated at time 3 hours in "macro cracks" of the (1/16th)fragment of the pellet; *Rigth*: Comparison of the model with experimental laboratory data (González-Robles, 2011) on radionuclide release from SNF pellet (normalised to unity) and model prediction assuming that 40 % of total tracer mass is initially associated with "macro cracks

The main contribution of the modelling efforts are the outcome of the model developments, coupling of non-saturated flow with radionuclide transport, estimation of the different kinetic release of the radioelements from the fuel samples as well as quantification of the elemental distribution in the rod after the irradiation phase.

First-Nuclides Database

Within the documentation activities of WP5 of the project, one of the important outcomes has been the compilation of a database containing all information available in the literature on IRF data. In this last version of the State of the Art report, data generated in the project has been also included in the database.

The main aim of the *IRF Database* development (Valls et al., 2014) is to make available all dissolution based fast/instant release data achieved within CP FIRST-Nuclides as well as previously published data. The data are compiled and can be used both for scientific purposes and for application in safety analyses. The studies compiled in the database have been performed under different experimental conditions, using different type of fuels, different sample preparations and different solutions.

A detailed description of the database is given in Appendix III of this report, where the organization of the database, the type of data included and all the features on how to use it for data analyses and plotting are described.

The objective of the database is to serve as a tool for analysing the data and it is the aim that it is used and continuously updated with the new appearing data.

The support of the database is an excel spreadsheet which is available upon request. As indicated more details are found in Appendix III.

6. Acknowledgement

The research leading to these results has received funding from the European Union's European Atomic Energy Community's (Euratom) Seventh Framework Programme FP7/2007-2011 under grant agreement n° 295722 (FIRST-Nuclides project).

7. References

Assmann, H. (1986) Advantages of oxidative UO_2 sintering process "NIKUSI", in: European Nuclear Society Meeting, Geneva 1986.

Assmann, H., Peehs, M., Roepenack, H. (1988) Survey of binary oxide fuel manufacturing and quality control, Journal of Nuclear Materials, 153, 115-126.

Bai, J.B., Prioul, C., Francois, D. (1994) Hydride Embrittlement in ZIRCALOY-4 Plate: Part I. Influence of Microstructure on the Hydride Embrittlement in ZIRCALOY-4 at 20 °C and 350 °C, Metallurgical and Materials Transactions A, 25A, 1168.

Bastide, B., Morel, B., Allibert, M. (1993) Nuclear fuel elements comprising a trap for fission products based on oxide, in, Uranium, Pechiney (Courbevoie, FR), United States.

Bel, J., Van Cotthem, A., De Bock, C. (2005) Construction, operation and closure of the Belgian repository for long-lived radioactive waste, in: 10th International Conference on Environmental Remediation and Radioactive Waste Management (ICEM 2005), Glasgow, UK, 2005.

Blair, P. (2008). Modelling of fission gas behaviour in high burn-up nuclear fuel. PhD Thesis, École Polytechnique Fédérale de Lausanne.

Blair, P. (2008) Modelling of fission gas behaviour in high burn-up nuclear fuel, in, École Polytechnique Fédéral, Lausanne, CH, 2008.

Chan, K.S. (1996) A micromechanical model for predicting hydride embrittlement in nuclear fuel cladding material, Journal of Nuclear Materials, 227, 220-236.

Clarens, F., González-Robles, E., Gimenez, F.J., Casas, I., de Pablo, J., Serrano, D., Wegen,D., Glatz, J.P., Martinez-Esparza, A. (2009) Effect of burn-up and high burn-up structure on spent nuclear fuel alteration, in: Publicación técnica 04-2009, Enresa, Madrid, Spain, pp. 177.

Cox, B. (1990) Pellet clad interaction (PCI) failures of zirconium alloy fuel cladding - A review. Journal of Nuclear Materials, 172, 249-292.

Craeye, B., Schutter, G.D., Humbeeck, H.V., Cotthem, A.V. (2008) Concrete containers for containment of vitrified high-level radioactive waste: The Belgian approach, in: M.G. Alexander, H.-D. Beushausen, F. Dehn, P. Moyo (Eds.) Second International Conference on Concrete Repair, Rehabilitation and Retrofitting (ICCRRR 2008), Cape Town, South Africa, November 2008., Taylor & Francis Group, London, Cape Town, South Africa, November 2008.

Curti, E., Froideval-Zumbiehl, A., Martin, M., Bullemer, A., Günther-Leopold, I., Puranen, A., Jädernäs, D., Roth, O., Grolimund, D., Borca, C.N., Velea, A. (2014b). X-Ray Absorption

Spectroscopy of Selenium in High-Burn-up UO_2 Spent Fuel form the Leibstadt and Oskarshamn-3 Reactors. Final Workshop Proceedings of the 7th EC FP CP FIRST-Nuclides Project (eds. Kienzler et al.).

Curti, E., Günther-Leopold, I., Linder, H.-P., Milosavljevic, N. (2014a). Results of Leaching Experiments on Spent UO_2 and MOX Nuclear Fuel Carried out at PSI. Final Workshop Proceedings of the 7th EC FP CP FIRST-Nuclides Project (eds. Kienzler et al.).

Deshon, J., Hussey, D., Kendrick, B., McGurk, J., Secker, J., Short, M. (2011) Pressurized Water Reactor Fuel Crud and Corrosion Modelling. Journal of Minerals, Metals and Material Society (JOM), 63, 64-72.

Dörr, W., Lansmann, V. (2007) Fuel pellet for a nuclear reactor and method for the production thereof, in, AREVA NP GmbH (Freyeslebenstrasse 1, 91058 Erlangen, DE), EUROPÄISCHE PATENTSCHRIFT.

Ferry C., Piron J. P., Poulesquen A., Poinssot C. (2007). Radionuclides release from the spent fuel under disposal conditions: Re-Evaluation of the Instant Release Fraction, in: Scientific Basis for Nuclear Waste Management, Sheffield, UK, 2007.

Fors, P., Carbol, P., Van Winckel, S., Spahiu, K. (2009) Corrosion of high burn-up structured UO_2 fuel in presence of dissolved H_2, Journal of Nuclear Materials, 394, 1-8.

Fors, P. (2009) The effect of dissolved hydrogen on spent nuclear fuel corrosion, in: Department of Chemical and Biological Engineering, Nuclear Chemistry, Chalmers University of Technology, Göteborg, pp. 132.

Forsyth, R. (1997) An Evaluation of Results from the Experimental Programme Performed in the Studsvik Hot Cell Laboratory, in, Svensk Kärnbränslehantering AB, Stockholm, Sweden, pp. 81.

Forsyth, R.S., Werme, L.O. (1992) Spent fuel corrosion and dissolution. Journal of Nuclear Materials, 190, 3-19.

Fuel suppliers/designers (2004), Fuel design data, Nuclear Engineering International, 48, 26-34.

Glatz, J.P., Giménez, J., Bottomley, D. (1999) Leaching of high burn-up UO_2 and MOX fuel rods with pre-set cladding defects, in: WM'99 Conference, 1999.

González-Robles, E. (2011) Study of Radionuclide Release in commercials UO_2 Spent Nuclear Fuels, in: Departament d'Ingenyeria Quimica, Universitat Politècnica de Catalunya, Barcelona, pp. 137.

González-Robles, E., Lagos, M., Bohnert, E., Müller, N., Herm, M., Metz, V., Kienzler, B. (2014). Leaching Experiments with Cladded Pellet and Fragments of High Burn-Up Nuclear

Fuel Rod Segment under Argon/H_2 Atmosphere. Final Workshop Proceedings of the 7th EC FP CP FIRST-Nuclides Project (eds. Kienzler et al.).

Gradel, G., Dörr, W. (2004) Method of producing a nuclear fuel sintered body, in, Framatome ANP GmbH (Erlangen, DE), United States.

Graf, R., Filbert, W. (2006) Disposal of Spent Fuel from German Power Plants - Paperwork or Technolgy, in: TopSeal 2006, Olkiluoto, Finland, 17 - 20 September 2006.

Grambow B., Bruno J., Duro L., Merino J., Tamayo A., Martin C., Pepin G., Schumacher S., Smidt O., Ferry C., Jegou C., Quiñones J., Iglesias E., Villagra N.R., Nieto J.M., Martínez-Esparza A., Loida A., Metz V., Kienzler B., Bracke G., Pellegrini D., Mathieu G., Wasselin-Trupin V., Serres C., Wegen D., Jonsson M., Johnson L., Lemmens K., Liu J., Spahiu K., Ekeroth E., Casas I., de Pablo J., Watson C., Robinson P. and Hodgkinson D. (2010) Final Report of the Project MICADO: Model uncertainty for the mechanism of dissolution of spent fuel in nuclear waste repository.

Gray, W.J., Wilson, C.N. (1995) Spent fuel dissolution studies FY 1991 to 1994, in, Pacific Northwest National Laboratory, Richland, Washington, USA, 1995.

Gray, W.J. (1999) Inventories of I-129 and Cs-137 in the gaps and grain boundaries of LWR spent fuels, in: D.J. Wronkewiecz, J.H. Lee (Eds.) Scientific Basis for Nuclear Waste Management XXII, Materials Research Society Symposium Proceedings, pp. 478-494.

IAEA (2001) Nuclear fuel behaviour modelling at high burn-up and its experimental support, in: Technical Committee, Windermere, United Kingdom, 19-23 June 2000.

Johnson L.H., Tait J.C. (1997) Release of segregated nuclides from spent fuel. SKB Technical Report TR-97-18.

Johnson L., Ferry C., Poinssot C. and Lovera P. (2005) Spent fuel radionuclide source-term model for assessing spent fuel performance in geological disposal. Part I: Assessment of the instant release fraction. Journal of Nuclear Materials, 346, 56-65.

Johnson L., Günther-Leopold I, Kobler Waldis J., Linder H. P., Low J., Cui D., Ekeroth E., Spahiu K., Evins L. Z. (2012) Rapid aqueous release of fission products from high burn-up LWR fuel: Experimental results and correlations with fission gas release. Journal of Nuclear Materials 420, 54-62.

Johnson L., Poinssot C., Ferry C. and Lovera P. (2004) Estimates of the instant release fraction for UO_2 and MOX fuel at t=0, in: A Report of the Spent Fuel Stability (SFS) Project of the 5th Euratom Framework Program, NAGRA Technical Report 04-08, Wettingen, Switzerland.

Kim, S.S., Kang, K. C., Choi, J. W., Seo, H. S., Kwon S. H., Cho. W. J. (2007) Measurement of the gap and grain boundary inventories of Cs, Sr and I in domestic used PWR Fuels, Journal of the Korean Radioactive Waste Society, 5, 79-84.

Kleykamp, H., Paschoal, J. O., Pejsa, R., Thümmler, F. (1985) Composition and structure of fission product precipitates in irradiated oxide fuels: Correlation with phase studies in the Mo-Ru-Rh- Pd and BaO-UO_2-ZrO_2-MoO_2 systems. J. Nucl. Mater. 130, 426.

Ledergerber, G., Abolhassani, S., Limbäck, M., Lundmark, R.J., Magnusson, K.A. (2008) Characterization of High Burn-up Fuel for Safety Related Fuel Testing. Journal of Nuclear Science and Technology, 43, 1006–1014.

Loida, A., Grambow, B., Kelm, M. (1999) Abgebrannter LWR-Kernbrennstoff: Auslaugverhalten und Freisetzung von Radionukliden. Abschlußbericht BfS-Projekt 9G213532100 (FZK-INE 009/99), pp. 147.

Lovera P., Férry C., Poinssot C. and Johnson L. (2003) Synthesis report on the relevant diffusion coefficients of fission products and helium in spent nuclear fuel, in, CEA, Direction de L'Énergie Nucléaire, Département de Physico-Chimie, Service d'Études du Comportement des Radionucléides Saclay, 2003.

Lucuta, P.G., Matzke, H. Hastings, I.J. (1996) A pragmatic approach to modelling thermal conductivity of irradiated UO_2 fuel: Review and recommendations, Journal of Nuclear Materials, 232, 166-180.

Marchal, N., Campos, C., Garnier, C. (2009) Finite element simulation of Pellet-Cladding Interaction (PCI) in nuclear fuel rods, Computational Materials Science, 45, 821-826.

Martínez-Torrents, A., Sureda, R., de Pablo, J., Clarens, F., Serrano-Purroy, D., Aldave de las Heras, L., Casas, I. (2014). Corrosion Test of Commercial UO_2 BWR Spent Nuclear Fuel for Fast/Instant Release Studies. Final Workshop Proceedings of the 7th EC FP CP FIRST-Nuclides Project (eds. Kienzler et al.).

Mccoy, J.K. (2010) Process for manufacturing enhanced thermal conductivity oxide nuclear fuel and the nuclear fuel, in, AREVA NP Inc. (Lynchburg, VA, US), United States, 2010.

Mennecart, T., Lemmens, K., Cachoir, C. (2014). Characterisation and Leaching Tests for the Experimental Determination of IRF Radionuclides for Belgian High-Burn-up Spent Nuclear Fuel. Final Workshop Proceedings of the 7th EC FP CP FIRST-Nuclides Project (eds. Kienzler et al.).

NEA (2006) Very High Burn-ups in Light Water Reactors, OECD/NEA, Paris, F, 2006.

Nucleonica GmbH. (2011). Nucleonica Nuclear Science Portal (www.nucleonica.com), Version 3.0.11.

Oversby, V.M., Shaw, H.F. (1987) Spent fuel performance data: An analysis of data relevant to the NNWSI project, in, Lawrence Livermore National Laboratory Report UCID-20926.

Pastore, G. (2012). Modelling of Fission Gas Swelling and Release in Oxide Nuclear Fuel and Application to the TRANSURANUS Code. Doctoral Thesis, Politecnico de Milano.

Poinssot C., Ferry C., Kelm M., Granbow B., Martínez A., Johnson L., Andriambolona Z., Bruno J., Cachoir C., Cavendon J. M., Christensen H., Corbel C., Jégou C., Lemmens K., Loida A., Lovera P., Miserque F., de Pablo J., Poulesquen A., Quiñones J., Rondinella V., Spahiu K. and Wegen D. H. (2005) Spent fuel stability under repository conditions – Final report of the European (SFS) project, in, Commissariat à l'énergie atomique (CEA), France.

Poinssot, C., Gras, J.-M. (2009) Key scientific issues related to the sustainable management of the spent nuclear fuel in the back-end of the fuel cycle, in: N.B.B. Robert J. Finch (Ed.) Scientific Basis for Nuclear Waste Management XXXII, Mat. Res. Soc. Symp. Proc., Boston, USA, 2009.

Puranen, A., Granfors, M., Roth, O. (2014a) Laser Ablation Study of Irradiated Standard UO_2 Fuel and Al/Cr Doped UO_2 Fuel. Final Workshop Proceedings of the 7th EC FP CP FIRST-Nuclides Project (eds. Kienzler et al.).

Puranen, A., Granfors, M., Roth, O. (2014b) Aqueous Leaching of ^{79}Se from Spent Nuclear Fuel. Final Workshop Proceedings of the 7th EC FP CP FIRST-Nuclides Project (eds. Kienzler et al.). WP3 Overview Final Workshop Proceedings - 7th EC FP - FIRST-Nuclides

Quiñones, J., Cobos, J., Iglesias, E., Martínez-Esparza, A., Van Winckel, S., Glatz, J.P. (2006) Preliminary approach obtained from Spent Fuel Leaching experiments performed by ITU-ENRESA/CIEMAT, in, CIEMAT, Madrid, Spain, pp. 27.

Rashid, J.Y.R., Yagnik, S.K., Montgomer, R.O. (2011) Light Water Reactor Fuel Performance Modeling and Multi-Dimensional Simulation. Journal of Minerals, Metals and Material Society (JOM), 63, 81-88.

Roth, O., Askeljung, C., Puranen, A., Granfors, M., Cui, D., Low, J. (2014b) Leaching of High Burn-up Spent Fuel With and Without Matrix Dopants. Final Workshop Proceedings of the 7th EC FP CP FIRST-Nuclides Project (eds. Kienzler et al.).

Roth, O., Puranen, A., Askeljung, C., Cui, D. (2014a) Selection of Materials and Characterization of Samples Used in Spent Fuel Leaching and Laser Ablation Studies. Final Workshop Proceedings of the 7th EC FP CP FIRST-Nuclides Project (eds. Kienzler et al.).

Roudil, D., Jégou, C., Broudic, V., Muzeau, B., Peuget, S., Deschanels, X. (2007) Gap and grain boundaries inventories from pressurized water reactors spent fuels, Journal of Nuclear Materials, 362, 411-415.

Roudil, D., Jegou, C., Broudic, V., Tribet, M. (2009) Rim instant release radionuclide inventory from French high burn-up spent UOX fuel, Materials Research Society Symposium Proceedings 1193, 627-633.

Rudling, P., Adamson, R., Cox, B., Garzarolli, F., Strasser, A. (2008) High burn-up fuel issues, Nuclear Engineering and Technology, 40.

Serrano, J.A., Rondinella, V.V., Glatz, J.P., Toscano, E.H., Quiñones, J., Díaz-Arocas, P.P., García-Serrano, J. (1998) Comparison of the Leaching Behaviour of Irradiated Fuel, SIMFUEL, and Non-Irradiated UO_2 under Oxic Conditions, Radiochimica Acta, 82, 33-37.

Serrano-Purroy D., Clarens, F., González-Robles, E., Glatz, J.P., Wegen, D.H., de Pablo, J., Casas, I., Giménez, J., Martínez-Esparza, A. (2012) Instant release fraction and matrix release of high burn-up UO_2 spent nuclear fuel: Effect of high burn-up structure and leaching solution composition, Journal of Nuclear Materials 427, 249–258.

Serrano-Purroy, D., Aldave de las Heras, L., Van Winckel, S., Martínez Torrents, A., Sureda, R., Glatz, J.P., Rondinella, V.V. (2014) WP3. Dissolution Based Release, IRF Corrosion Tests of Commercial UO2 BWR Spent Nuclear Fuel. Final Workshop Proceedings of the 7th EC FP CP FIRST-Nuclides Project (eds. Kienzler et al.).

Slonszki, E., Hózer, Z. (2014) Isotopes Dissolution during Wet Storage of Damaged and Leaking VVER fuel. Final Workshop Proceedings of the 7th EC FP CP FIRST-Nuclides Project (eds. Kienzler et al.).

Smailos, E. (2000) Influence of welding and heat treatment on corrosion of a high-level waste container material carbon steel in disposal salt brines. Corrosion Science, 56, 1071-1074

Sneyers, A. (2008) Understanding and Physical and Numerical Modelling of the Key Processes in the Near Field and their Coupling for Different Host Rocks and Repository Strategies (NF-PRO), in, SCK•CEN, Brussels.

Stan, M. (2009) Multi-scale models and simulations of nuclear fuels. Nuclear Engineering and Technology, 41, 39-52.

Stan, S. (2004) Prediction of Nuclear Fuel Materials Properties, in: Transactions, American Nuclear Society, pp. 131-133.

Stehle, H., Assmann, H. Wunderlich, F. (1975) Uranium-Dioxide Properties for LWR Fuel Rods. Nuclear Engineering and Design, 33, 230-260.

Tverberg, T. (2007) Mixed-oxide (MOX) Fuel Performance Benchmark: Summary of the Results for the Halden Reactor Project MOX Rods, OECD/NEA, Paris, F, 2007.

TVO, Nuclear power plant units Olkiluoto 1 and Olkiluoto 2, in, TVO Nuclear Services Oy, Olkiluoto, FI-27160 EURAJOKI, FINLAND.

Valls, A., Duro, L., González-Robles, E. (2015) IRF Database. Excel file available at CP FIRST-Nuclides webpage: www.firstnuclides.eu

Van Uffelen, P., Konings, R.J.M., Vitanza, C., Tulenko, J. (2010) Analysis of Reactor Fuel Rod Behavior, in: D.G. Cacuci (Ed.) Handbook of Nuclear Engineering, Springer Science+Business Media LLC, pp. 1519-1627.

Van Uffelen P., Pastore G., Di Marcello V., Luzzi L. (2011). Multiscale modelling for the fission gas behaviour in the Transuranus code. Nuclear Engineering and Technology 43, 477-488.

Varias, A.G., Massih, A.R. (2000) Simulation of hydrogen embrittlement in zirconium alloys under stress and temperature gradients, Journal of Nuclear Materials, 279, 273-285.

Wilson, .C.N., Shaw, H.F. (1987) Experimental study of the dissolution of spent fuel at 85 °C in natural groundwater, in: J.D. Bates, W.B. Seefeldt (Eds.) Scientific Basis for Nuclear Waste Management X, Materials Research Society Symposium Proceedings, pp. 123-130.

Wilson, C.N. (1987) Results from Cycles 1 and 2 of NNWSI Series 2 Spent Fuel Dissolution Tests, in, HEDL-TME 85-22 UC-70, Westinghouse Hanford Company.

Wilson, C.N. (1990) Results from NNWSI Series 2 bare fuel dissolution tests. , in: Pacific Northwest Laboratory Report, PNL-7169, Richland, Washington, USA, 1990.

Wilson, C.N. (1988) Summary of results from the series 2 and series 3 NNWSI bare fuel dissolution test, in: M.J. Apted, R.E. Westerman (Eds.) Scientific Basis for Nuclear Waste Management XI, Materials Research Society Symposium Proceedings, pp. 473.

Wilson, C.N., Gray, W.J. (1990) Measurement of soluble nuclide disolution rates from spent fuel, in: M.J. Apted, R.E. Westerman (Eds.) Scientific Basis for Nuclear Waste Management XIII, Materials Research Society Symposium 112, pp. 473.

Zwicky, U., Low, J., Ekeroth, E. (2011) Corrosion Studies with High Burn-up Light Water Reactor Fuel, in, SKB TR-11-03, Svensk Kärnbränslehantering AB, Stockholm, Sweden, 2011, pp. 84.

Appendix I: Manufacturers of UO_2 fuel and fuel elements

Nuclear fuel elements are produced for energy production in nuclear power plants. The fuels to be considered in the CP FIRST-Nuclides are uranium oxide fuels having initial ^{235}U enrichments up to 4.3 wt.%. An overview of fuel elements for the different types of reactors was published by Fuel suppliers (2004) The nuclear fuel used in Europe is mainly produced by subsidiaries of AREVA or Westinghouse.

FBFC (French acronym for Franco-Belgian Fuel Fabrication), a subsidiary of AREVA comprises three sites at Romans (F), Pierrelatte, Tricastin (F), and Dessel (B). The **Romans site** transforms uranium hexafluoride supplied by EURODIF into uranium oxide powder (UO_2). It also fabricates uranium pellets, rods, nozzles, and fuel assemblies for pressurized water reactors (PWRs). FBFC Romans employs 830 persons. The **Pierrelatte site** manufactures support grids for assemblies for PWR fuels and Harmoni™ control clusters. These products are then supplied to the Romans and Dessel plants, which fabricate fuel assemblies. It also produces spacers for MELOX's MOX fuel assemblies. **FBFC International** located in **Dessel**, Belgium, produces fuel assemblies for pressurized water reactors. The plant also fabricates pellets with gadolinium, rods, plugs, and spring packs for fuel assemblies for pressurized water reactors and boiling water reactors. It also assembles the various components for MOX fuel assemblies. At the Tricastin site, EURODIF Production operates the Georges Besse plant performing uranium enrichment by gaseous diffusion. With the new Georges Besse II plant in operation since 2009, AREVA uses the centrifugation technology for enrichment.

Advanced Nuclear Fuels GmbH (ANF) is a full subsidiary of AREVA. Its headquarters are in Lingen (Germany) and its operations are distributed over three sites in Germany. The plant in **Lingen** produces UO_2 powder, as well as pellets, rods, and fuel assemblies for pressurized and boiling water reactors. Since the site's commissioning in 1977, it has produced more than 20,000 fuel elements. Following stages in assembly fabrication are performed at the Lingen plant: uranium hexafluoride (UF_6) is transformed into uranium oxide (UO_2). This oxide is compacted into cylindrical pellets and baked in ultra-high-temperature furnaces. The pellets are then stacked into tubes of around 4 meters in length, called "rods". These are then sealed off at the ends. The zirconium-alloy rod cladding is subjected to rigorous testing. The rods are grouped into assemblies with the appropriate dimensions.

Westinghouse Sweden Nuclear Fuel Factory, situated in Västerås, Sweden. The fuel factory manufactures fuel assemblies for PWRs and BWRs, and fuel channels and control rods for BWRs. The factory in Västerås is responsible for the entire chain from research and development to manufacturing of nuclear fuel, as well as for control rods and fuel channels for BWR plants including codes for core surveillance. The present fuel factory has been in operation since 1971 and was continuously expanded and modernized. The factory produces approximately 400 tons of UO_2 fuel for BWRs and PWRs per year. In the conversion of UF_6 into UO_2 powder, the capacity as well as the plant license is limited to 600 tons UO_2.

British Nuclear Fuels Ltd (BNFL) was the manufacturer fuel elements feeding the British Energy's (BE) AGR reactors as well as BNFL's own Magnox Reactors. Advanced gas-cooled reactor fuel (AGR) comprises of 36 stainless steel rods each containing 64 pellets, grouped together inside a graphite 'sleeve' to form a 'fuel assembly'. BNFL also made fuel for the older Magnox Reactors which consists of a natural uranium metal bar with a magnesium alloy casing. BNFL's core expertise for fuel manufacture was based on fabrication of the uranium pellets, and the final assembly of the fuel elements. BNFL was finally abolished in 2010.

Appendix II: Canister/disposal concepts

Germany

In Germany, the disposal concept for spent nuclear fuel, the so called "direct disposal of spent fuel" was developed and examined with respect to safety aspects. The reference concept is based on the triple purpose cask POLLUX for transport, storage and final disposal as well as a conditioning technique that separates fuel rods from the structural parts of the fuel assemblies. Another most promising option is called BSK 3-concept. Both concepts are described in the literature (Graf and Filbert, 2006). The POLLUX canister consists of a shielding cask with a screwed lid and an inner cask with bolted primary and welded secondary lid. The inner cask consists of fine-grained steel 15 MnNi 6.3, the thickness of the cylindrical wall is 160 mm according the mechanical and shielding requirements. The outer cask provides shielding. Its thickness is 265 mm and it consists of cast iron GGG 40 (DIN 1693-1/2 steel grade). The weight of the inner cask (including spent fuel is 31 ton, the weight of the outer cask is 34 ton. Ten complete fuel elements can be packed into a POLLUX cask. Another possibility is the accommodation of consolidated fuel rods (5.4 tHM). The BSK 3 cask was designed for accommodation of consolidated fuel rods. The capacity of a BSK 3 is designed for three PWR fuel elements or nine BWR fuel elements. The wall thickness of the BSK 3 is 50 mm.

Sweden

The Swedish/Finish Canister concept bases on an insert of nodular iron (a kind of cast iron) which is inserted into a copper tube (Figure A - 1). The copper lids are welded by friction stir welding. The canisters are about 5 meters long and have a diameter of more than one meter. When the canister is filled with 12 spent fuel elements, it weighs between 25 and 27 metric tons. (SKB Brochure “Encapsulation, When, where, how and why?”).

Belgium

In Belgium, the Supercontainer was developed which surrounds the steel cask containing the fuel elements by a thick concrete overpack (Bel et al., 2005). The supercontainer is intended for the disposal of (vitrified) high level heat-emitting waste and for the disposal of spent fuel assemblies. In this concept, the spent fuel assemblies are enclosed in a carbon steel overpack of about 30 mm thick. This overpack has to prevent contact of the waste with the water coming from the host formation during the thermal phase of several 1000 years for the spent fuels assemblies. For corrosion protection, the overpack is enveloped by a concrete buffer of about 70 cm thickness. The concrete is surrounded by a stainless steel cylindrical envelope (called liner). The outside radius of the supercontainer for spent fuel assemblies is about 1.9 m, and a length of about 6 m, it’s mass is about 54 tons (Craeye et al., 2008).

Figure A - 1. Components of the Swedish canister concept at SKB's Canister Laboratory in Oskarshamn.

In all three concepts, corrosion of the fine-grained steel 15 MnNi 6.3 (Germany), nodular iron (Sweden, Finland) or carbon steel (Belgium) is a prerequisite before groundwater may come into contact with the fuel. Different corrosion processes may therefore be relevant. The three examples listed above all show a general corrosion due to an active corrosion mechanism. Only in the Belgian case, a passivation of the steel may occur. Under the reducing conditions of a deep underground disposal, anaerobic corrosion of the steel takes place. This active corrosion process normally shows a non-uniform reduction of the canister thickness, especially if there are gradients in material or mineralogical composition or in the welding material. The degree of non-uniformity in thickness reduction of the actively corroding steels was observed to be a factor of 2, in comparison to the general corrosion rate (Smailos, 2000). However, in the case of a heat-affected zone close to a welding, the corrosion rate may increase. For example, Figure A - 2 shows the corrosion of the welding of fine-grained steel in $MgCl_2$ brine at 150°C under γ-irradiation (10 Gy/h).

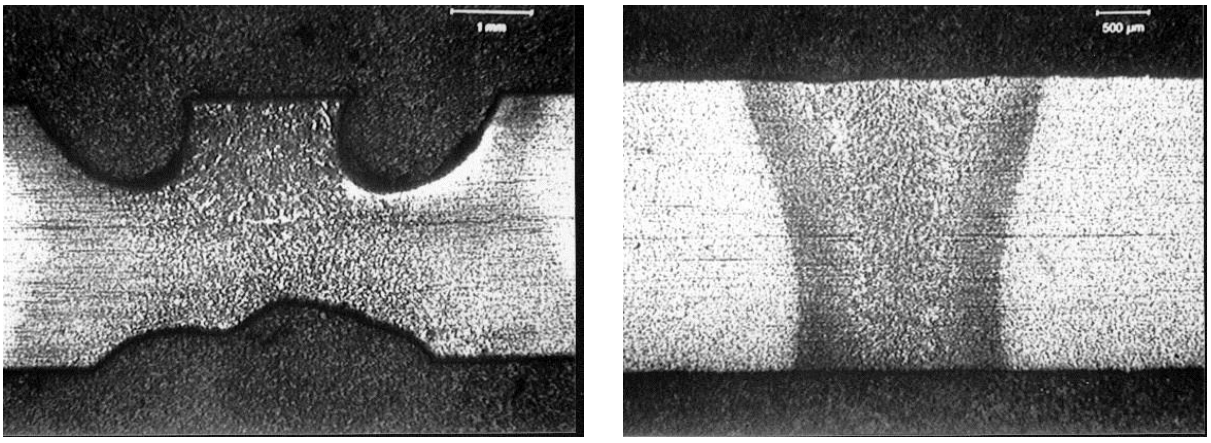

Fine-grained steel welding, untreated *Fine grained steel, heat-treated*

Figure A - 2: Corrosion of the welding of fine-grained steel 1.0566 (FStE 355) in $MgCl_2$ brine at 150°C under γ-irradiation (10 Gy/h) (Smailos, 2000).

Appendix III: IRF database

The annex is focused on presenting and describing the "*IRF Database"* developed by Amphos21 in collaboration with all the beneficiaries of the FIRST-Nuclides project. This database is available at the project website (www.firstnuclides.eu).

This document is the user guide of the *IRF Database*.

Introduction and objectives

The Deliverable D5.1 – State of the Art report is the main outcome of the documentations task within WP5 of the FIRST-Nuclides project. The first version of the State-of-the-Art was reported at the beginning of the project and it provides a view on basic information related with the spent nuclear fuel and the IRF studies done in the past decades. A description of different type of spent fuels, processes induced during SF irradiation or the modelling tools used for fuel performance are included in the basic information section. The second part of the report includes a summary of more than 100 published experiments which have used different samples, experimental techniques, experimental conditions, type of solutions, etc. This report has been updated after the second year of the project.

The final version of this deliverable not only includes an update of the report with a summary of the results obtained in the project, extensively reported in the different deliverables, annual workshop proceedings and final scientific report (D.5.13), but also a database compiling data on fast/instant release fraction (IRF) of relevant radionuclides from the spent fuel. This database is called "*IRF Database*".

The main aim of the *IRF Database* development is to make available all dissolution based fast/instant release data achieved within CP FIRST-Nuclides as well as previously published data. The data are compiled and can be used both for scientific purposes and for application in safety analyses. The studies compiled in the database have been performed under different experimental conditions, using different type of fuels, different sample preparations and different solutions.

The IRF Database

The *IRF Database* compiles the studies carried out during the last decades on the fast/instant release of relevant radionuclides from spent nuclear fuel. Dissolution based fast/instant release data obtained from the experimental work performed in the frame of the CP FIRST-Nuclides project are also included and can be easily identified.

The database is developed in excel format and it consists on a single excel file which is made up of several inter-linked spreadsheets. Figure A - 3 shows the sections the *IRF Database* is composed of:

i. detailed information of publications

ii. summary table

iii. data processing

iv. references

Several spreadsheets are focused on providing detailed information obtained from the selected publication (*(i)* in Figure A - 3). The summary table (*(ii)* in Figure A - 3) is created from those spreadsheets of the detailed information sections and it is a summary that includes the basic parameters and the IRF results for each sample included in the database. All the information form the summary table are used to create the Processing data spreadsheet (*(iii)* in Figure A - 3) where the user can process and plot the results. Finally, a forth section consist on a single spreadsheet with the list of references (*(iv)* in Figure A - 3). More information on each of the mentioned sections can be found in the following sections.

Figure A - 3: Scheme of the IRF Database organization

i. Detailed information

Several spreadsheets are included in this section; one spreadsheet for each publication included in the database. These spreadsheets are highlighted in orange and are called considering the year of publication and the first author (e.g. 1995_Gray or 2012_Jonhson).

Each spreadsheet is divided in two different sections, the first one focused on providing detailed information of the experimental conditions for each of the studied samples (i.e. sample treatment, analysis techniques, solution composition…) and a second one presenting the results and the corresponding uncertainties, in case they are available.

Information on experimental conditions

The left-hand side of the spreadsheet is composed by 6 different tables aimed on providing detailed information on (i) spent fuel characteristics, (ii) sample preparation, (iii) experimental conditions, (iv) solution composition, (v) analysis techniques and (vi) results.

Each column of the table corresponds to one sample and rows provide sample information (see Figure A - 4). When data is not provided in the publication, the row is highlighted in grey.

- ***Spent Fuel***

	SFR1-Pl	SFR2-Pl	SFR3-a-Pl	SFR3-b-Pl	SFR1-Pw	SFR2-Pw	SFR3-a-Pw	SFR3-b-Pw
Material	UOX							
Reactor type	PWR							
Reactor name								
BU (GWd/tHM)	39.6	35	45.9	65.9	39.6	35	45.9	65.9
Fuel Power (W/cm)								
FGR (%)	0.5	0.22	5		0.5	0.22	5	
Info available	initial enrichment, cooling time							

Figure A - 4: Example of the type of tables included in the "Detailed information" spreadsheets, section of "Information on experimental conditions".

The parameters included in these tables as well as its description are presented below (see Table A - 1 to

Table A - 6).

Table A - 1: *Spent fuel*: properties of the spent nuclear fuel material used for sample preparation.

Parameter	Description
Material	Type of spent nuclear fuel (UO_2 or MOX)
Reactor type	Type of reactor where the fuel has been irradiated (mainly, PWR or BWR)
Reactor name	Name of the reactor where the fuel has been irradiated
BU calculated	Burn-up of the spent fuel calculated using specific software
Fuel Power (W/cm)	Fuel power rate of the spent fuel

FGR (%)	Fission gas release
Info available	Other information that is available at the publication with respect to the spent fuel characteristics

Table A - 2: *Sample:* information on the preparation of the sample and its characteristics.

Parameter	Description
Sample type	Type of sample prepared: - Pellet: according to the production process - Segment: cuts through the middle planes of pellets - Slice: cut through a single pellet - Fragment: piece or portion of fuel - Powder: fuel material obtained after declad, sieving and milling - Cladding with attached fuel. - Bare fuel: segment with an artificially produced defect
Cladding	It is specified if the sample contains the cladding or not. When detached is specified, SF and detached clad are used in the experiment.
Preparation	Description of the methodology followed during the sample preparation
Sample size (mm or µm)	Size of the sample. - Fragments, pellets and bare fuel: it refers to the height and diameter of the sample in mm - Powder: it is the particle size in µm.
Sampled region	Region of the spent fuel sampled. It can be sample the whole spent fuel or selecting either the center or the rim zone.
Surface area	Surface are of the sample in m^2/g
Mass in experiment	Amount of sample (in gram) used in the experiment
I0 calculation	Software used to calculate the initial inventory. In the case, the inventory is also measured, it is specified.
Info available	Other information that is available at the publication with respect to the sample characteristics

Table A - 3: *Experiment:* conditions under the experiments have been undertaken.

Parameter	Description
Batch/column	Experimental method: batch or column
Kind of experiment	Experimental method details: complete replenishment or not of the solution, static or dynamic leaching tests, etc.
Duration experiment	Duration of the experiment
Atmosphere	Under which type of atmosphere the experiments have been conducted (e.g. anoxic, H_2, open air, etc.).
Carbonated system	Presence or not of carbonates in the solution
Ox/red	Experimental conditions: oxidizing, reducing…

Parameter	Description
Sample pre-treatment	Description of the sample pre-treatment process in case it has exist
Info available	Other information that is available at the publication with respect to the experimental conditions

Table A - 4: *Solution:* characteristics of the solution used for the leaching experiments.

Parameter	Description
Solution comp	Composition of the solution
Volume	Volume of solution used for the experiment
pH	pH of the solution
pO_2	pH of the solution
Eh	pH of the solution
T°	Temperature the experiments were carried out
Other	Other relevant information on the characteristics of the solution

Table A - 5: *Analysis:* techniques used for the analysis of both the spent fuel sample and the solution.

Parameter	Description
Samples filtered	Description if the samples are filtered before being analysed and the filter size
Anal. techniques (solid)	Techniques used for the analysis of the spent fuel sample
Anal. techniques (solution)	Techniques used for the analysis of the solution

Table A - 6: *Results:* techniques used for the analysis of both the spent fuel sample and the solution.

Parameter	Description
IRF contribution area	Probable location of the radionuclides released: gap or gran boundaries. Generally, studies using fragment/pellet/bare fuel samples are looking at the gap contribution while powder sample studies are focused on grain boundaries contribution.
Measured FGR (%)	Fission gas released measured during the experiment
Results & calculation meth.	Description of the results provided in the publication and how they are calculated.
Data origin	It is specified if the data presented in the database is directly obtained from tables or if they are extrapolated from a figure.
Ouput time series	Time series where samples have been taken and analysed
Time evolution	It is specified if the author has publish IRF/FIAP/FNU evolution with time
Diss rate U	Value of the dissolution rate of uranium obtained from the experiments, in case it has been calculated
Other results provided	List of other results that are provided in the publication

Results

The right-hand side of the spreadsheet aims on presenting the obtained results. Original data from the publication is included either as a table or graph.

In case data are presented in a graphic format, it is also included the extrapolated values which are used in the "summary table" and "data processing" spreadsheets. It is also detailed the origin of the extrapolated data:

a) data have been extrapolated by the database authors or

b) data have been previously extrapolated and published by other authors (in this case the reference of the publication is included).

When the publication contains additional results that may be of interest for the user, they are also included in this section (e.g. FIAP evolution with time, data on uranium, etc.).

Data uncertainties are presented in this section when they are included in the publication but they are not included in the "summary table" spreadsheet.

Figure A - 5 shows an example of the results section where not only IRF values are provided but also the cumulative IRF evolution of caesium.

- ***Instant release fraction (%)***

	Area	Xe	Cs		Sr		I	
SFR1	gap	0.5	0.25	±0.05	0.03	±0.01	< 0.2	
SFR2	gap	0.22	0.65	±0.03	0.03	±0.01	< 0.2	
SFR3-a	gap	5	0.85	±0.10	0.21	±0.10	2.2	±1.00
SFR3-b	gap	5	1.7	±0.20	0.21	±0.10	3.6	±1.50
SFR1	GB	0.5	1.3-2.7		0.3	±0.10	< 0.2	
SFR2	GB	0.22	0.2	±0.05	0.09	±0.02	< 0.2	
SFR3-a	GB	5	0.2	±0.05	0.06	±0.02	< 0.4	
SFR3-b	GB	5	0.2	±0.05	0.06	±0.02	< 0.4	

- ***Cumulative IRF (%)***

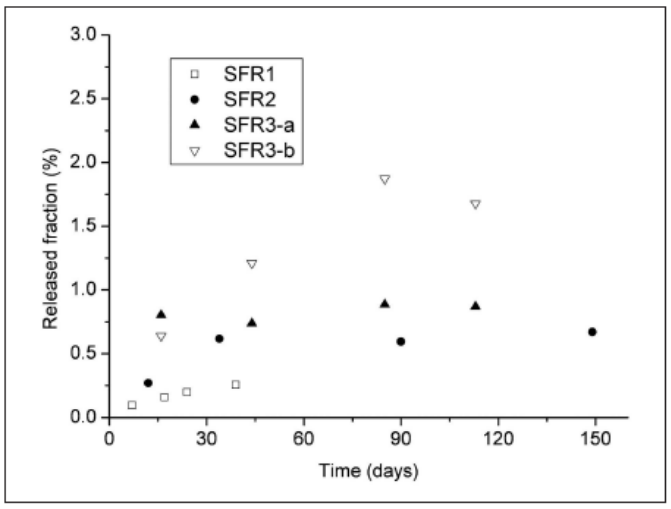

Fig. 1. Cumulated fraction of the cesium released from the used fuels in distilled water.

Figure A - 5: Example of the results that can be included in the "results" sub-section of the "detailed information" spreadsheets.

ii. Summary table

This spreadsheet aims on summarizing the information provided at the "detailed information" spreadsheets in a single table that includes the whole amount of samples considered in this database.

The organization of the table is showed in Figure A - 6. Each row represents a single sample and columns stand for the basic information related with the samples. As it can be seen in Figure A - 6; information is organized by issue (each colour one issue): (i - purple) spent fuel from which the sample has been taken, (ii - orange) information on the sample itself, (iii - green) experimental conditions under the sample has been studied, (iv - red) solution

used for the study, (v - blue) results obtained for each specific sample and (vi - grey) reference where the study is published in.

	Spent fuel **P1 P2 …**	*Sample* **P1 …**	*Experimental conditions* **P1 P2 …**	*Solution* **P1**	*Results* **P1 P2 …**	*Reference* **P1 …**
Sample 1						
Sample 2						
Sample 3						
…						
Sample n						

Figure A - 6: Scheme of the summary table organization.

Each of the included samples is identified in two different ways:

a) *Author ID:* it stands for the name the authors of the study gave to each of the samples. The same name for different samples of the database can be found.

b) *Database ID:* these identifications have been included in order to not have duplicates on sample names. In general, author ID is used but when duplicates are found the database ID consist on the author ID plus an identification of what differs among them.

The parameters reported in the summary table are presented in Figure A - 7 as a function of the issue they describe.

Spent fuel	***Sample***	***Experimental conditions***	***Solution***	***Results***	***Reference***
- SF - Reactor Type - BU (GWd/tHM) - Fuel power (W/cm) - FGR (%)	- Sample type - Cladding - Sample size (mm or µm) - Region sampled	- Experiment duration (days) - Atm. - Carbonated system - Temperature (°C)	- Solution composition	- Measured FGR (%) - Type of data - Origin of data - Cs (%) - Sr (%) - I (%) - Rb (%) - Tc (%) - Mo (%)	- Ref. - Year - FIRST-Nuclides data? - Detailed info - Results

Figure A - 7: Parameters include in the "SummaryTable" spreadsheet as a function of what they describes.

iii. *Data processing*

"DataProcessing" spreadsheet (Figure A - 8) allows the treatment and analysis of data by means of plotting numerical data (parameters and/or results) and providing basic information of plotted samples in order to analyse possible reasons for outliers.

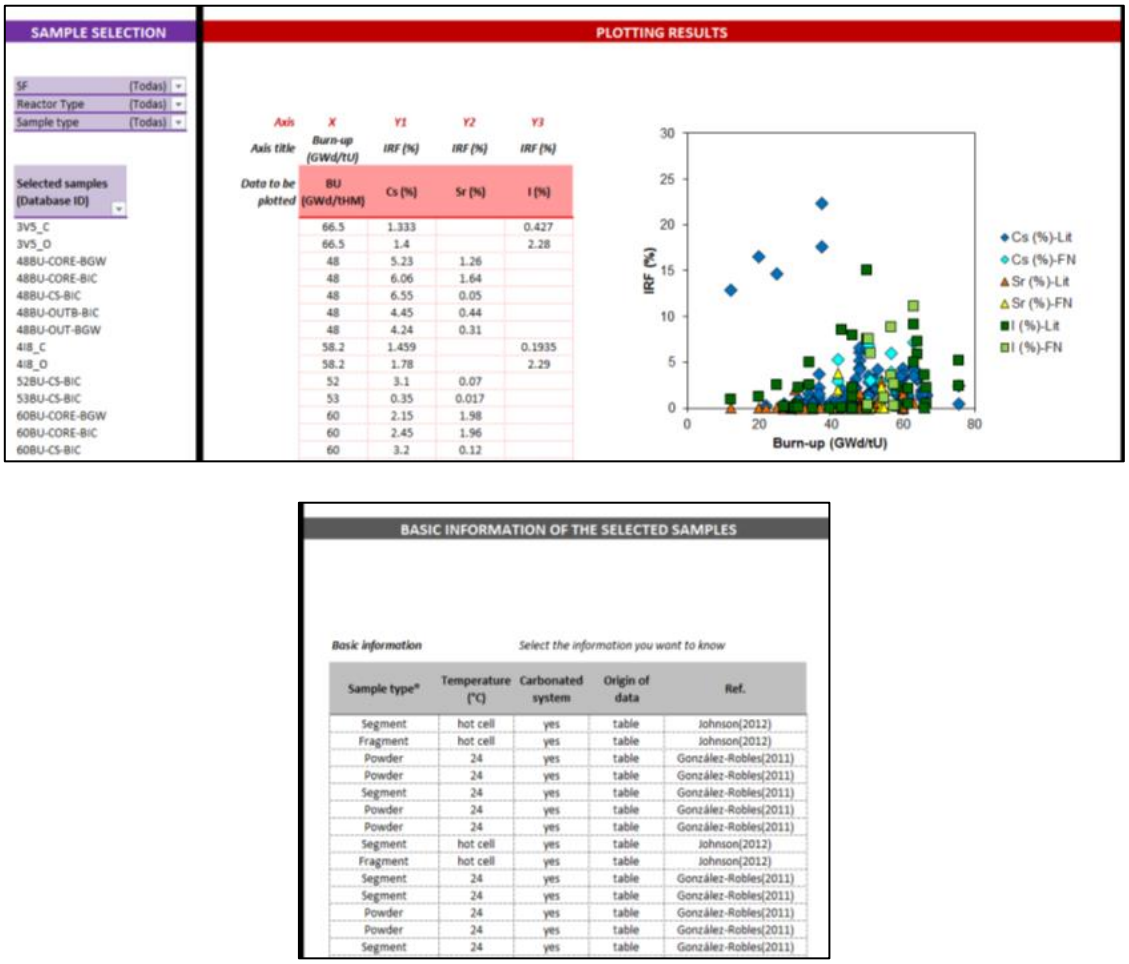

Figure A - 8: Screenshot of the "Graphic" spreadsheet.

The way this spreadsheet should be used is presented below.

1. Sample selection (purple section in Figure A - 8): Selection of the samples which results are desired to be plotted. Samples can be sorted by spent fuel material (UOX or MOX), type of reactor (PWR or BWR) and sample preparation (pellet, segment, powder, etc.).
2. Plotting results (red section in Figure A - 8): the user selects the parameters to plot for both X and Y axis. It can be plotted up to 3 parameters in the Y axis. The graph is automatically updated with the selected data. Axis units are also updated when changing the parameters to be plotted.

Note 1: A drop down list must be used to select the parameters to be plotted (X and Y axis)

Note 2: FIRST-Nuclides data is showed in a lighter colour. Data published before the project are plotted as dark blue, dark green and dark orange symbols and data obtained in FIRST-Nuclides studies are shown as light blue, light green and light orange symbols.

3. Basic information of the selected samples (grey section in Figure A - 8): the user selects via a drop down list the parameters of the summary table to be shown.

iv. Reference

The last spreadsheet of the database is the list of references used in the database. In the case of FIRST-Nuclides data, information on the performed investigations can be found in the project deliverables and the three editions of the Annual Workshop Proceedings. All CP FIRST-Nuclides documentation can be found at the project webpage (www.firstnuclides.eu).

Conclusions

A database compiling data on fast/instant release fraction (IRF) of relevant radionuclides from the spent fuel published and generated during the FIRST-Nuclides project has been developed by Amphos21 with the collaboration of all FIRST-Nuclides beneficiaries.

The *IRF Database* has been presented at the Final Workshop of the project (1-2 September 2014, Karlsruhe, Germany) and it received a good feedback from the attendees.

The database will not be updated regularly with future publications related with IRF estimation but it will be updated in case new data from experiments started during the FIRST-Nuclides project are available. The last version of the database will be available at the project webpage (www.firstnuclides.eu).